Earth Critical Zone 3 (2026) 100079

Contents lists available at ScienceDirect

Earth Critical Zone

journal homepage: www.sciencedirect.com/journal/earth-critical-zone

Limestone mining coproducts enhance soil pH and micronutrient availability in tropical sugarcane systems

Marlon Rodrigues[a,*], Carlos Augusto Posser Silveira[b], Everson Cezar[c], Glaucio Leboso Alemparte Abrantes dos Santos[d], Leticia Romagna[a], Marcos Rafael Nanni[d]

[a] Department of Biological and Environmental Sciences, Federal Technological University of Paraná, Medianeira, Paraná, Brazil
[b] Embrapa Temperate Climate, Pelotas, Rio Grande do Sul, Brazil
[c] Department of Agricultural and Earth Sciences, University of Minas Gerais State, Passos, Minas Gerais, Brazil
[d] Department of Agronomy, University of Maringá State, Maringá, Paraná, Brazil

HIGHLIGHTS

- Acidic soil corrected with industrial by-products.
- Mn availability reduced by 60% after liming.
- Sugarcane yield maintained at 88–128 Mg ha^{-1}
- Rhythmite and limestone improved soil fertility.
- Circular economy approach for waste valorization.

GRAPHICAL ABSTRACT

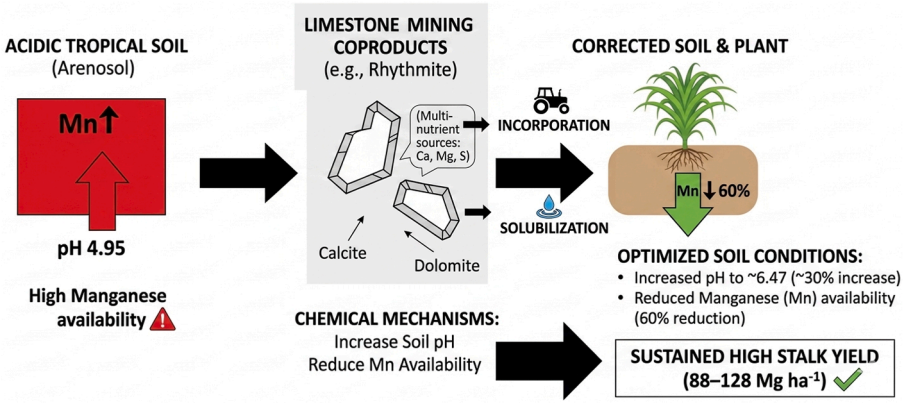

ARTICLE INFO

Keywords:
Coproducts
Micronutrient availability
Mineralogy
Soil fertility
Sugarcane nutrition
Tropical soils

ABSTRACT

This study evaluated the effects of contrasting limestone coproducts used as Ca–Mg–S sources, combined with different potassium (K) fertilizer sources, on soil chemical attributes, micronutrient dynamics, and plant performance in a sugarcane system. A split-plot field experiment was conducted during plant cane and ratoon cycles, with soil sampling at two depths (0–20 and 20–40 cm) to determine pH and extractable Cu, Fe, Mn, and Zn, as well as leaf micronutrient accumulation and stalk yield. Limestone coproducts significantly increased soil pH relative to the control, with maximum increases of up to 30%, particularly under rhythmite-based and combined limestone–rhythmite treatments. These amendments reduced extractable Mn concentrations by up to 60% in the surface layer. Linear mixed-effects models showed significant main effects of crop cycle and soil depth on Fe and Zn contents ($p < 0.01$), while cycle × depth interactions were not significant. Potassium source selection had no consistent effect on soil chemical attributes. Leaf micronutrient accumulation and stalk yield were not affected by limestone coproducts or K sources, with stalk yield ranging from approximately 88 to 128 Mg ha^{-1} across crop cycles. Multivariate analyses revealed strong separation among treatments based on soil chemical attributes,

* Corresponding author.
E-mail address: marlonr@utfpr.edu.br (M. Rodrigues).

https://doi.org/10.1016/j.ecz.2026.100079
Received 2 February 2026; Received in revised form 24 April 2026; Accepted 25 April 2026

driven mainly by soil pH and Fe–Mn availability, whereas plant variables showed limited differentiation. Overall, limestone mining coproducts acted as effective multinutrient amendments, improving soil chemical conditions without inducing short-term changes in plant nutritional status or yield, supporting their use as sustainable tools for long-term soil fertility management in sugarcane systems.

1. Introduction

Soil fertility is a central determinant of agricultural productivity and sustainability, reflecting the soil's capacity to supply essential nutrients in adequate amounts and in an appropriate balance over time while maintaining chemical conditions conducive to root development and nutrient uptake. In tropical agroecosystems, this balance is particularly fragile due to the dominance of highly weathered soils, intense rainfall, and strong leaching processes, which collectively promote soil acidification and depletion of exchangeable base cations (Dong et al., 2022; Rodrigues et al., 2021b). In warm and humid climates, soils in tropical and subtropical regions naturally undergo acidification due to intense weathering and leaching processes, with base cations (Ca^{2+}, Mg^{2+}, K^{+}, Na^{+}) being leached from the soil exchange complex when excess rainfall containing soil organic acids and dissolved CO_2 passes down the soil profile (Liu et al., 2025). Consequently, effective soil amendment strategies are indispensable to sustain crop performance, especially in high-demand systems such as sugarcane cultivation (Ofoe et al., 2023).

Sugarcane production in tropical regions, notably in Brazil, is largely concentrated on acidic soils rich in iron and aluminum oxides but deficient in calcium (Ca^{2+}), magnesium (Mg^{2+}), and, in many cases, sulfur (S) (Borges et al., 2020). Land in Brazil is dominated by intensely weathered soils characterized by high acidity, low macronutrients, and high metal and aluminum (Al) bioavailability, which often represents a stress condition for crop plants (Labanca et al., 2020). Soil acidity correction through liming has therefore become a foundational practice in sugarcane management, with well-documented benefits for soil chemical quality, root system development, and crop longevity across successive ratoon cycles (Thorburn et al., 2011).

Traditionally, soil acidity correction relies on conventional limestone materials produced specifically for agricultural use. However, growing attention has been directed toward coproducts generated by mining and mineral processing activities, particularly limestone coproducts, as alternative soil amendments. These materials, often derived from quarrying, crushing, and beneficiation processes, are frequently underutilized or disposed of despite their substantial chemical and mineralogical potential (Russell et al., 2024; Salgado et al., 2024). From an agronomic perspective, limestone mining coproducts may represent valuable resources for sustainable soil management, offering a dual benefit of improving soil fertility while promoting the circular use of mineral resources (de Carvalho Ribeiro et al., 2025; Rodrigues et al., 2021c, 2023).

Recent comprehensive reviews demonstrate that soil remineralization using rock powders derived from mining and industrial by-products has gained attention as a sustainable strategy to restore degraded soils, improve fertility, and reduce reliance on synthetic fertilizers (Burbano et al., 2022; de Carvalho Ribeiro et al., 2025; Rodrigues et al., 2024b). These materials, rich in nutrients and beneficial minerals, also offer potential for carbon sequestration and contribute to circular economy practices by repurposing byproducts into agricultural inputs (Luthra et al., 2022; Skov et al., 2024).

Unlike conventional agricultural lime, limestone coproducts can exhibit distinct mineralogical compositions, particle size distributions, and degrees of reactivity, depending on their geological origin and processing history (du Toit et al., 2024; Manning, 2018; Manning and Theodoro, 2020). These characteristics influence not only their capacity to neutralize soil acidity but also their ability to supply a broader range of nutrients. In addition to Ca and Mg, many mining coproducts contain trace amounts of micronutrients such as iron (Fe), manganese (Mn), zinc (Zn), and copper (Cu), which may become agronomically relevant under certain soil conditions (Barreto et al., 2024; de Carvalho Ribeiro et al., 2025; Richardson, 2024). Consequently, these materials should not be viewed solely as acidity correctives, but rather as multinutrient amendments capable of modulating soil chemical equilibria and micronutrient dynamics (van Straaten, 2007).

The agronomic relevance of such coproducts is particularly pronounced in tropical systems, where micronutrient availability is strongly regulated by soil pH and redox conditions (Goulding, 2016; Holland et al., 2018). In acidic soils, elements such as Mn and Fe may reach excessive concentrations, posing toxicity risks, whereas Zn and Cu deficiencies can occur due to strong adsorption onto oxide surfaces (Silva et al., 2024). Below pH 5.2, manganese concentrations can reach phytotoxic levels, particularly in highly weathered Ultisols and Oxisols typical of tropical regions (Huang et al., 2016). Amendments that alter soil pH and base saturation inevitably influence the solubility, speciation, and plant availability of these micronutrients. Limestone coproducts, through their liming effect and mineralogical composition, therefore have the potential to reshape micronutrient dynamics beyond the immediate supply of base cations (Barreto et al., 2024; Rodrigues et al., 2024b).

Despite their potential, the agronomic performance of limestone mining coproducts remains insufficiently documented under field conditions, especially with respect to their influence on micronutrient dynamics and plant nutritional status. Most studies focus on conventional liming materials, while fewer investigations explicitly address coproducts with heterogeneous mineralogy and reactivity in the field (Li et al., 2019). Moreover, the interaction between such materials and fertilizer sources, including potassium inputs applied in split-plot arrangements, is rarely explored in long-term or multi-cycle experiments.

We hypothesized that (i) limestone coproducts with contrasting mineralogical characteristics would differentially affect soil pH and micronutrient availability across soil depths (addressed in Section 3.2); (ii) interactions between Ca–Mg–S coproducts and potassium sources would influence soil chemical balance without necessarily altering yield responses (addressed in Sections 3.2 and 3.3); and (iii) residual effects of these mining-derived amendments would persist into the ratoon cycle, contributing to sustained improvements in soil chemical conditions while maintaining plant nutritional stability (addressed in Sections 3.2, 3.3, and 3.4). By addressing these hypotheses, this study aims to advance the understanding of mining coproducts as viable tools for sustainable soil fertility management in tropical sugarcane systems.

2. Materials and methods

2.1. Coproducts characterization

The input materials were collected from a 15 m–thick stratigraphic profile overlying a limestone deposit located in the municipality of Tietê, São Paulo State, Brazil (22°55′5.52″ S; 47°46′1.68″ W; WGS84) (Fig. 1). Based on petrographic classification, the limestone mining coproducts are identified as limestone and rhythmite, both belonging to the Irati Formation, and clayey siltstone, derived from the Corumbataí Formation.

The total micronutrient contents of the input materials (Table 1) were determined by inductively coupled plasma optical emission spectrometry (ICP-OES) at Acme Analytical Laboratories Ltd. (Acmelabs), Vancouver, Canada, using the LF200 analytical protocol based on lithium borate fusion. The presence of potentially toxic heavy metals in rhythmite and clayey siltstone was evaluated by inductively coupled plasma–atomic emission spectrometry (ICP-AES), following the Environmental Protection Agency procedures described by Martin et al.

(1992). All measured concentrations complied with the limits established by current Brazilian environmental legislation (Brasil, 2016).

The particle size distribution of the input materials was classified as powder, with 100% of particles < 2.00 mm, 70% < 0.84 mm, and 50% < 0.30 mm, resulting in a theoretical reactivity of 68%. The mineralogical composition of the coproducts was determined by X-ray diffraction (XRD). Samples were finely ground in a porcelain mortar to particle sizes <0.074 mm, mounted on aluminum sample holders, and analyzed using an X-ray diffractometer (Shimadzu XRD-6000) equipped with CuKα radiation. Diffraction patterns were collected in step-scanning mode over a 2θ range of 5–70°, with a step size of 0.02°, under Bragg–Brentano geometry (Testoni et al., 2022). Following the reading, the interpretation of the collected data was performed by comparison with reference standards from the International Center for Diffraction Data (Smith and Jenkins, 1996) using X'Pert HighScore Plus 2.0.1 software (PANalytical, 2002).

2.2. Chemical characterization of the soil

Prior to the establishment of the experiment, soil samples were collected from the 0–20 cm layer of an Arenosol (WRB., 2015) located at 22°58′36.83″ S and 52°28′25.34″ W for the characterization of clay content and baseline chemical attributes of the experimental area. The soil samples were oven-dried at 50 °C under forced air circulation until constant mass, then gently ground and passed through a 2 mm sieve. Soil chemical analyses included the determination of exchangeable Ca^{2+} and Mg^{2+} extracted with 1 mol L^{-1} KCl, sulfate-S ($S–SO_4^{2-}$) extracted with calcium phosphate, soil pH measured in $CaCl_2$ solution, and organic carbon determined by the wet oxidation method, following the methodologies proposed by Teixeira et al. (2017), whereas for P and K^+ (resin) were determined according to Moniz et al. (2009). Potential acidity was evaluated in an indirect way by the change in pH of the sample in relation to the SMP buffer (Shoemaker et al., 1961). After determination of the elements, we calculated the sum of bases (SB = Ca^{2+} + Mg^{2+} + K^+) and the potential capacity of cation exchange (CEC_p = SB + H^+ + Al^{3+}). Initial characterization of clay content and the chemical attributes of the soil is shown in Table 2.

Arenosols are characterized by coarse texture, low clay content (140 g kg^{-1} in this study), reduced cation exchange capacity, and limited pH buffering capacity, which render them particularly susceptible to acidification but also more responsive to liming amendments due to lower acid load and reduced sorption competition for base cations. The initial base saturation of 40% indicates moderate chemical fertility, placing the soil at the lower boundary of the adequate range for sugarcane production (Pauletti and Motta, 2017).

2.3. Design and experimental procedure

The study was conducted in an area of approximately 2000 m^2 at the experimental station of RIDESA (Interuniversity Network for the Development of the Sugar and Alcohol Sector) in Paranavaí, Paraná State, Brazil (Fig. 2). The area had been previously cultivated with *Brachiaria ruziziensis*. According to the Köppen climate classification, the region has a humid subtropical climate (Cfa), characterized by an

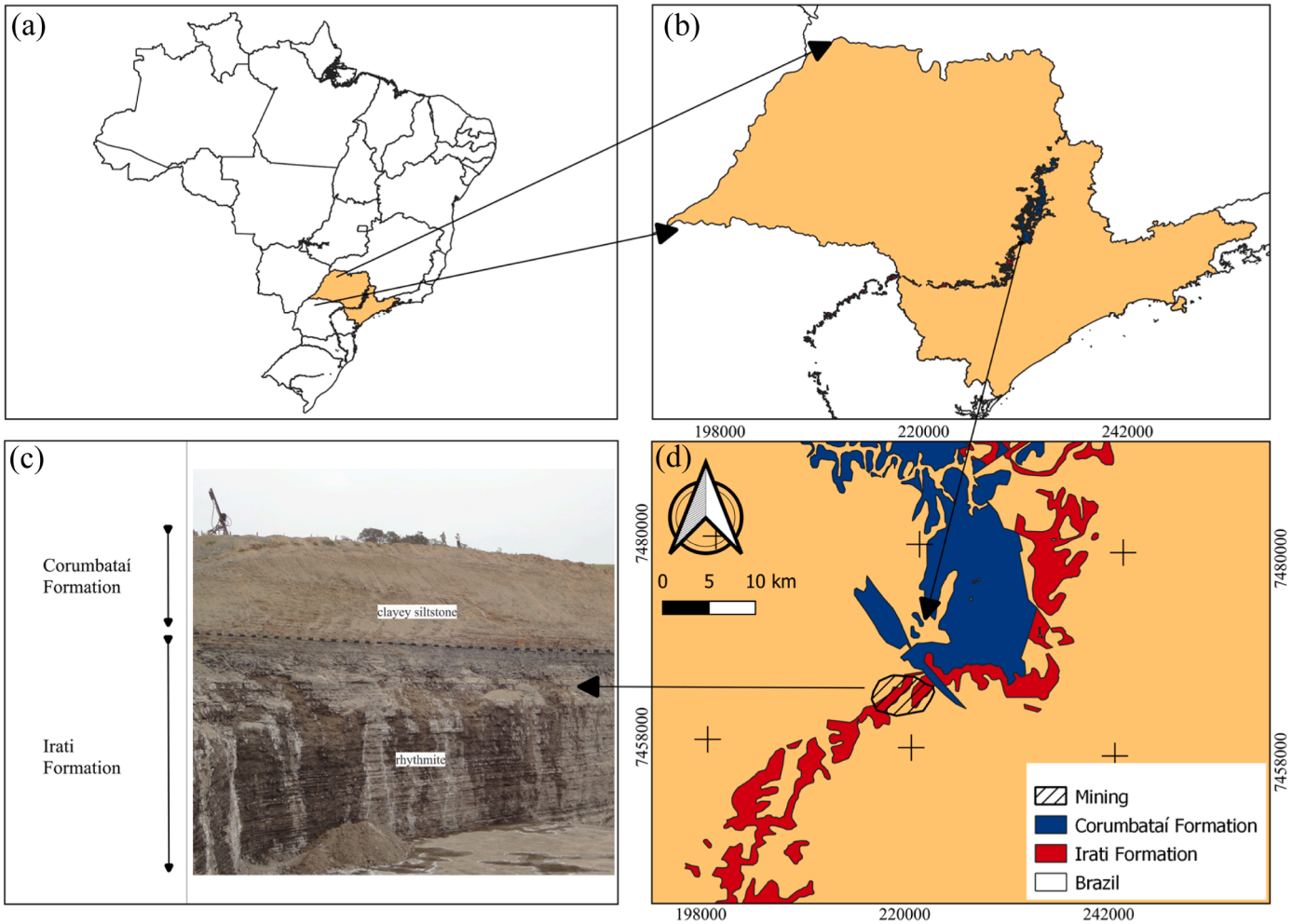

Fig. 1. Map of Brazil (a), state of São Paulo (b), stratigraphic profile for the collection of coproducts (c) and outcrop of the Corumbataí (CF) and Irati (IF) Formations.

average temperature of approximately 18 °C in the coldest month and 22 °C in the warmest month. The climate exhibits no distinct dry season, although rainfall is predominantly concentrated during the summer months (de Oliveira and Borrozzino, 2018). The soil class that prevails in the area is Arenosol (derived from the Caiuá Sandstone Formation).

The treatments were arranged in a split-plot arrangement in a randomized complete block design, with four replicates. Main plots (primary factor) consisted of five sugarcane rows, each 6.0 m long, spaced 1.50 m apart, with 2.0 m between adjacent plots, where Ca–Mg–S sources were applied. Subplots (secondary factor) were composed of five rows, each 3.0 m long, spaced 1.50 m apart, with 0.5 m between subplots, and received different K_2O sources. Treatments were defined according to the combination of Ca–Mg–S and K sources as follows: T1, control + phonolite; T2, control + clayey siltstone; T3, limestone + phonolite; T4, limestone + clayey siltstone; T5, rhythmite + phonolite; T6, rhythmite + clayey siltstone; T7, limestone + rhythmite + phonolite; T8, limestone + rhythmite + clayey siltstone; T9, limestone + gypsum + phonolite; T10, limestone + gypsum + clayey siltstone; T11, limestone + fidagran + phonolite; and T12, limestone + fidagran + clayey siltstone.

Input application rates followed the recommendations of the Fertilization and Liming Manual of the State of Paraná (Pauletti and Motta, 2017). Limestone, considered primarily a source of Ca and Mg, was applied to increase the sum of exchangeable Ca^{2+} and Mg^{2+} to 3 $cmol_c$ dm^{-3}. Gypsum, fidagran, and rhythmite, considered mainly sources of S, were applied at rates equivalent to a recommendation of 700 kg ha^{-1} of gypsum. Phonolite and clayey siltstone, used as K_2O sources, were applied at rates equivalent to 140 kg ha^{-1} of K_2O (Table 3).

Limestone was applied uniformly over the entire experimental area. The remaining inputs were applied in furrows at a depth of 0–20 cm, with rows spaced 1.5 m apart. For all treatments, triple superphosphate was applied at a rate of 200 kg ha^{-1} of P_2O_5 and urea at 70 kg ha^{-1} of N within the furrows, which were subsequently covered.

Immediately after input application, sugarcane (*Saccharum officinarum* L., cultivar RB867515) was planted using a pre-sprouted seedling system at a density of two plants per linear meter. Seven months after planting, all leaves from 15 plants per plot were collected, and 15 fully expanded +3 leaves were selected for the determination of Cu, Fe, Mn, and Zn concentrations, following the methodology described in Section 2.4. Leaf sampling at seven months after planting coincided with the grand growth phase of the plant cane cycle, a period of rapid vegetative expansion and high nutrient demand, which is considered the most representative stage for nutritional diagnosis in sugarcane (Silva, 2009). Fourteen months after input application, sugarcane was harvested, and soil samples were collected from the planting row at depths of 0–20 and 20–40 cm. Three subsamples per plot were collected and composited for the determination of soil pH ($CaCl_2$) and extractable Cu, Fe, Mn, and Zn using DTPA extraction (Moniz et al., 2009).

2.4. Sugarcane tissue analysis

The leaf samples collected at seven months of cultivation were oven-dried at 65 °C under forced air circulation until constant mass. Leaf dry matter yield per hectare was then estimated, and the macronutrient contents of the +3 leaves were determined following the methodology described by Silva (2009). For micronutrient analysis, plant tissue samples were subjected to nitroperchloric digestion, and the concentrations of Cu, Fe, Mn, and Zn were quantified using inductively coupled plasma atomic emission spectrometry (ICP-AES). Micronutrient accumulation was calculated as the product of leaf dry matter yield per hectare and the corresponding nutrient concentration, with results expressed in kg ha^{-1}.

2.5. Statistical analysis

Data were initially evaluated for normality and homoscedasticity using the Shapiro–Wilk and Levene tests, respectively. When necessary, data were log-transformed to meet the assumptions of parametric analyses. Data were analyzed using a split-plot analysis of variance (ANOVA) within a randomized complete block design. Ca–Mg–S sources were assigned to main plots, whereas K sources were allocated to subplots, with four replicates. Crop cycle (plant cane and ratoon) and soil depth (0–20 and 20–40 cm) were considered additional fixed factors in the model. For soil attributes, the ANOVA model included the effects of Ca–Mg–S source, K source, crop cycle, soil depth, and their interactions, using the appropriate error terms for main plots and subplots. For plant tissue attributes, the model included Ca–Mg–S source, K source, crop cycle, and their interactions. Block effects were considered random. When significant effects were detected, treatment means were compared using Tukey's honestly significant difference (HSD) test at a significance level of $p \leq 0.05$.

To further evaluate the robustness of treatment effects and account for the hierarchical structure of the experiment, linear mixed-effects models were additionally fitted, considering block as a random effect. The outcomes of these models were consistent with those obtained from the split-plot ANOVA and are presented as complementary information.

Multivariate analyses were applied to explore relationships among soil chemical attributes and plant responses. Principal component analysis (PCA) was performed separately for (i) soil pH and extractable micronutrients (Cu, Fe, Mn, and Zn) and (ii) stalk yield and leaf micronutrient accumulation. Prior to PCA, variables were standardized (mean = 0, standard deviation = 1) to avoid scale effects. PCA results were interpreted based on eigenvalues, variable loadings, and biplots. In addition, Pearson correlation coefficients were calculated among soil chemical attributes and plant variables, and the results were visualized using a correlation matrix heatmap to identify patterns of association and potential trade-offs among variables.

All statistical analyses and graphical representations were performed using Python, with packages including *pandas*, *numpy*, *scipy*, *statsmodels*, *scikit-learn*, *matplotlib*, and *seaborn*.

3. Results

3.1. Mineralogical description of the coproducts

The mineralogical composition of the coproducts used in this study is shown in Fig. 3. Rhythmite (Fig. 3a) was composed mainly of quartz, smectite, calcite, dolomite, and pyrite. Bituminous shale (Fig. 3b) contained quartz, albite, mica, and pyrite, whereas clayey siltstone (Fig. 3c) was characterized by the presence of smectite, illite, quartz, feldspar, and mica. These mineral assemblages are consistent with those reported in previous studies for similar lithologies (Goldberg and Humayun,

Table 1
Total micronutrients and heavy metals contents present in the coproducts used in the experiments.

Coproducts	MnO	Fe_2O_3	Zn	Cu	Cd	Pb	Hg	As
	%		mg kg^{-1}					
limestone[a]	0.20	0.76	11.0	4.8	<QL[c]	3.7	<QL[c]	3.60
rhythmite[a]	0.35	4.52	32.5	17.3	<QL[c]	15.11	<QL[c]	0.51
clayey siltstone[b]	0.09	5.37	70.0	25.3	0.20	18.50	0.07	3.90

Inductively coupled plasma optical emission spectrometry (ICP-OES), using a modified aqua regia digestion (1:1:1 HNO_3:HCl:H_2O); [a]Irati Formation; [b]Corumbataı' Formation; [c]quantification limit (Cd = 0.09; Hg = 0.02).

Table 2
Initial characterization of clay content and the chemical attributes of the arable layer (0-20 cm) of an Arenosol in Paranavaí/PR – Brazil.

Soil	Clay[a]	C	pH (H_2O)	pH ($CaCl_2$)	H + Al	Al	Ca	Mg	K	CEC_p	P	SO_4	V
	— g kg^{-1} —				——— $cmol_c$ dm^{-3} ———						- mg dm^{-3} -		%
Arenosol	140	4.84	6.0	5.0	2.05	0.05	0.72	0.51	0.10	3.38	4.2	6.4	40

[a] pipette method.

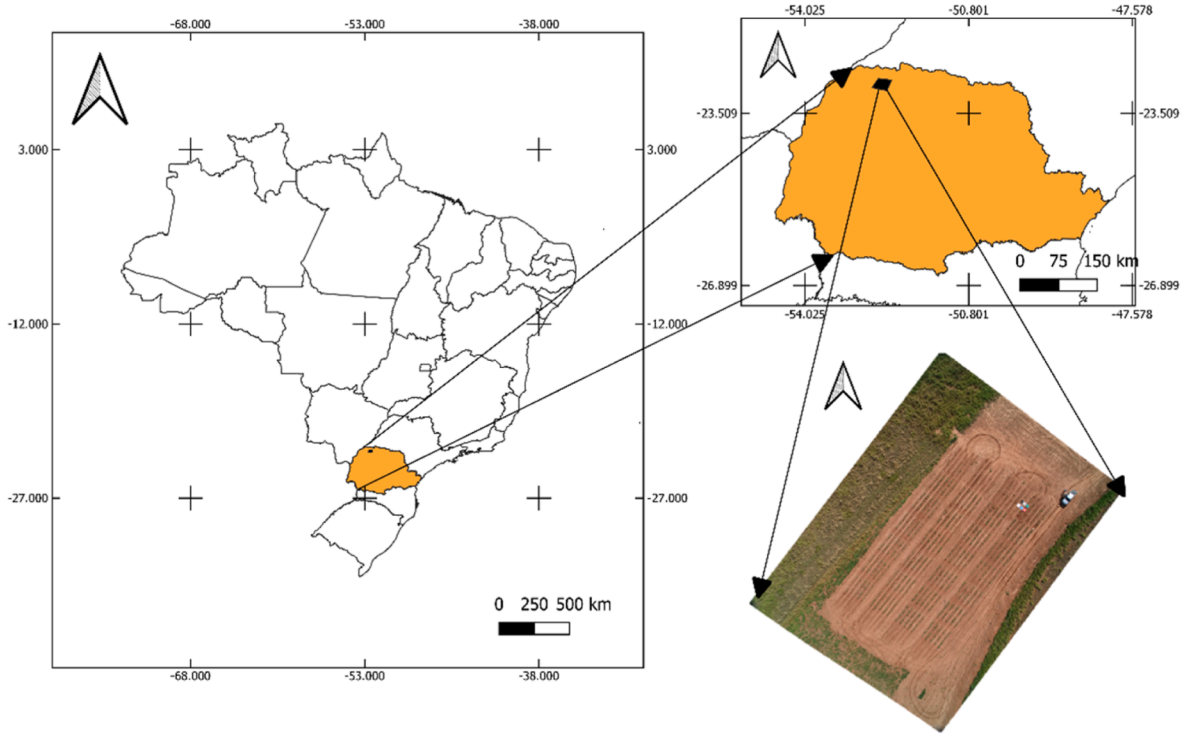

Fig. 2. Location map of the experimental area.

Table 3
Treatment factors and doses of the Ca, Mg, S and K_2O sources.

plot	supblot	treatments	doses (kg ha^{-1})			
			Ca	Mg	S	K_2O
control	phonolite[a]	T1	0	0	0	140
	clayey siltstone[a]	T2				
limestone[a]	phonolite[a]	T3	586	351	10	140
	clayey siltstone[a]	T4				
rhythmite[a]	phonolite[a]	T5	555	415	91	140
	clayey siltstone[a]	T6				
limestone[a]+ rhythmite[a]	phonolite[a]	T7	1141	766	101	140
	clayey siltstone[a]	T8				
limestone[a]+ gypsum[b]	phonolite[a]	T9	698	351	101	140
	clayey siltstone[a]	T10				
limestone[a]+ fidagran[c]	phonolite[a]	T11	914	479	101	140
	clayey siltstone[a]	T12				

[a] Rock powders.
[b] Industrial subproduct of the production of P-based fertilizers.
[c] Granulated material composed of $CaMg(CO_3)_2$ + $CaSO_4$ + S.

2016; Margarita Torres Moreno et al., 2014; Moreno-García et al., 2018) that demonstrate the presence of similar minerals to those found in this study in the evaluated rocks.

3.2. *Effect of the application of mining coproducts on soil chemical attributes*

During the plant cane cycle, soil chemical attributes in the 0–20 cm layer were significantly affected by Ca–Mg–S sources applied to the main plots, whereas K sources exerted a limited and inconsistent influence (Table 4). The statistical differences observed among treatments translated into clear shifts in soil fertility classes when interpreted according to Pauletti and Motta (2017), particularly for soil pH and Mn availability.

Soil pH differed significantly among Ca–Mg–S sources ($p \leq 0.05$), with the control treatments showing the lowest values (4.95–5.07), statistically inferior to all amended treatments. According to Pauletti and Motta (2017), these values fall within the low pH class, indicative of acidic conditions. The application of limestone, rhythmite, or their combinations significantly increased soil pH to values between 5.38 and 6.47, shifting the soil from the low to the medium or high pH classes. The

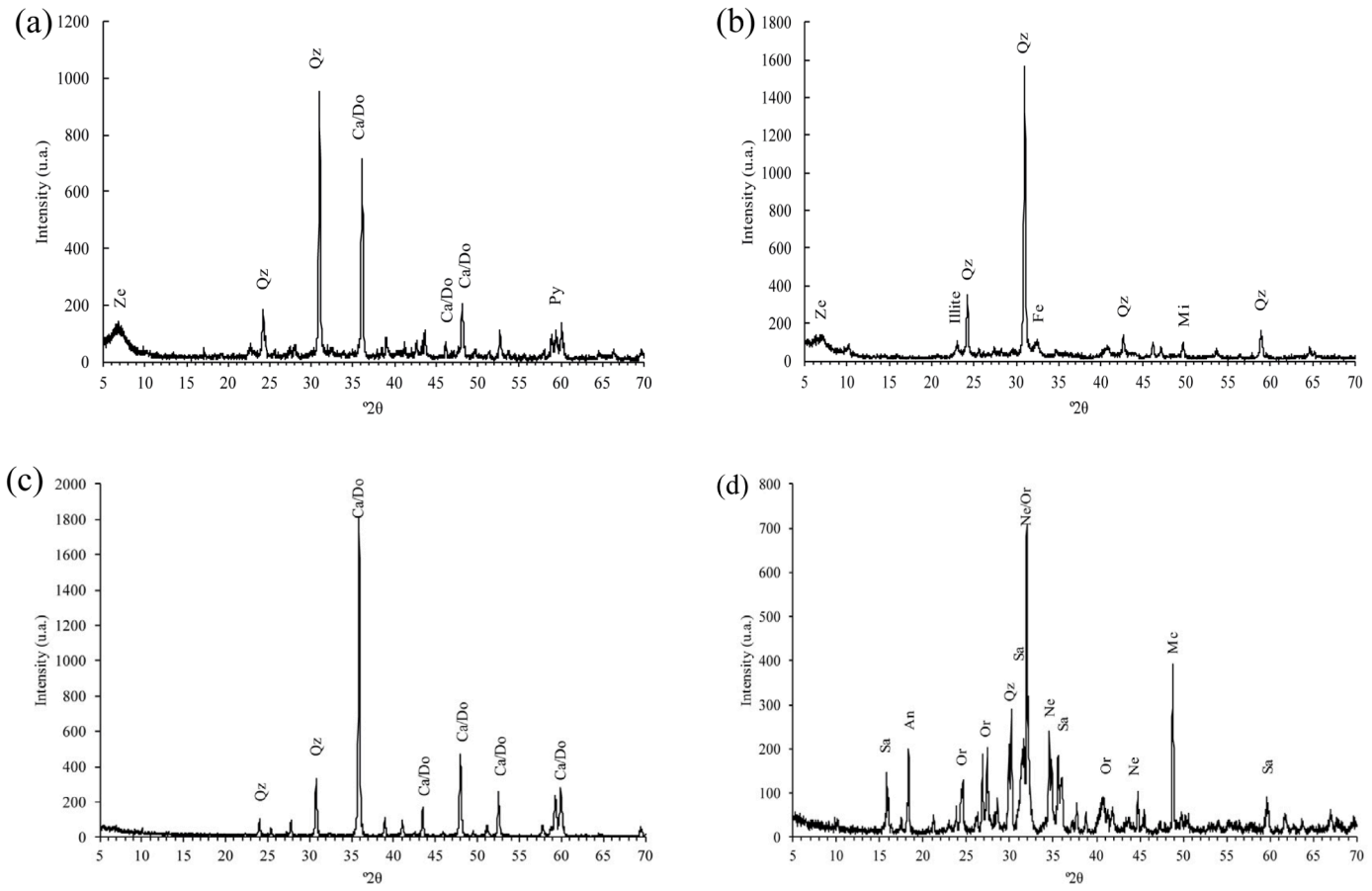

Fig. 3. X-ray diffractometry of rock powders used in the study: rhythmite (a), clayey siltstone (b), limestone (c) and phonolite (d); *Ca/Do = calcite and dolomite; Ze = zeolite; Qz = quartz; Fe = feldspar; Py = pyrite; Mi = mica; Sa = sanidine; An = analcime; Or = orthoclase; Ne = nepheline; Mc = microcline.

combined limestone + rhythmite treatment resulted in the highest pH values (6.40–6.47), which were statistically superior to single-source applications and classified as high, demonstrating a more effective acidity correction in the surface layer.

Exchangeable Cu contents did not differ statistically among Ca–Mg–S sources or between K sources ($p > 0.05$), remaining within a narrow range (1.03–1.35 mg kg^{-1}). All treatments were classified as high in terms of Cu availability, indicating that neither soil amendments nor K source selection altered Cu fertility status in the plant cane cycle.

Soil Zn contents also showed no significant differences among Ca–Mg–S sources ($p > 0.05$), with values ranging from 0.62 to 2.50 mg kg^{-1}. Agronomically, Zn levels were predominantly classified as medium to high, and no treatment resulted in Zn contents below the adequate range, even under treatments that significantly increased soil pH.

In contrast, soil Mn contents were strongly affected by Ca–Mg–S sources ($p \leq 0.05$). The control treatments exhibited the highest Mn contents (15.22–18.32 mg kg^{-1}), statistically superior to all amended treatments and classified as high, a range associated with increased risk of Mn toxicity under acidic conditions. All Ca–Mg–S amendments significantly reduced Mn concentrations to values between 8.38 and 13.48 mg kg^{-1}, shifting Mn availability from the high to the medium fertility class. The limestone + rhythmite treatments showed the greatest reductions, with Mn levels statistically lower than those observed under limestone or rhythmite applied alone, indicating a cumulative effect on Mn immobilization mediated by soil pH increase.

Soil Fe contents exhibited limited sensitivity to Ca–Mg–S sources,

Table 4
Mean soil pH and nutrient contents in the 0–20 cm layer as affected by treatments during the plant cane cycle.

Plots	Subplots	pH	Cu (mg kg^{-1})	Fe (mg kg^{-1})	Mn (mg kg^{-1})	Zn (mg kg^{-1})
Control	Clayey Siltstone	4.95 cA	1.35 aA	11.75 aA	18.32 aA	2.50 aA
Control	Phonolite	5.07 cA	1.30 aA	10.75 A	15.22 aA	1.12 aA
Limestone	Clayey Siltstone	5.38 bA	1.20 aA	10.50 aA	13.48 bA	0.80 aA
Limestone	Phonolite	5.85 bA	1.03 aA	6.75 aA	10.88 bA	1.00 aA
Rhythmite	Clayey Siltstone	6.05 bA	1.20 aA	8.50 aA	11.85 bA	0.87 aA
Rhythmite	Phonolite	5.85 bA	1.18 aA	7.50 aA	12.73 bA	1.33 aA
Limestone + Rhythmite	Clayey Siltstone	6.47 aA	1.12 aA	4.75 aA	8.70 bA	0.62 aA
Limestone + Rhythmite	Phonolite	6.40 aA	1.07 aA	5.25 aA	8.38 bA	0.92 aA
Limestone + Gypsum	Clayey Siltstone	5.42 bA	1.20 aA	8.50 aA	12.75 bA	1.70 aA
Limestone + Gypsum	Phonolite	5.88 bA	1.12 aA	6.25 aB	12.18 bA	1.60 aA
Limestone + Fidagran	Clayey Siltstone	5.72 bA	1.20 aA	8.00 aA	9.95 bA	0.85 aA
Limestone + Fidagran	Phonolite	5.65 bA	1.20 aA	8.00 aA	10.70 bA	1.20 aA

Means followed by the same lowercase letter do not differ among Ca–Mg–S sources (main plots), while uppercase letters indicate differences among K sources within each Ca–Mg–S source (subplots), according to Tukey's test ($p \leq 0.05$).

with most treatments not differing statistically ($p > 0.05$). Values ranged from 4.75 to 11.75 mg kg^{-1} and were classified as medium to high according to Pauletti and Motta (2017). A significant difference between K sources was observed only within the limestone + gypsum treatment, where clayey siltstone resulted in higher Fe contents than phonolite; however, this difference did not alter the Fe fertility class and is therefore of limited agronomic relevance.

Overall, Ca–Mg–S amendments improved soil chemical quality in the surface layer by raising pH and reducing Mn availability, without inducing Cu, Fe, or Zn deficiencies.

During the ratoon cane cycle, soil chemical attributes in the 0–20 cm layer remained significantly influenced by Ca–Mg–S sources applied to the main plots, whereas K sources exerted a limited effect on most variables (Table 5). The statistically significant differences observed among treatments were reflected in distinct soil fertility classes when interpreted according to Pauletti and Motta (2017), particularly for soil pH, Mn, and Fe availability (see Table 6).

Soil pH differed significantly among Ca–Mg–S sources ($p \leq 0.05$). Control treatments presented the lowest pH values (4.95–4.97), which were statistically inferior to all amended treatments and classified as low, indicating persistent soil acidity during the ratoon cycle. In contrast, Ca–Mg–S amendments increased soil pH to values ranging from 5.55 to 6.20, shifting the soil to the medium to high pH classes. The highest pH values were observed under the combined limestone + rhythmite treatments, which were statistically superior to single-source applications and classified as high, demonstrating the persistence of the liming effect into the ratoon cycle.

Exchangeable Cu contents were not significantly affected by Ca–Mg–S sources or K sources ($p > 0.05$), remaining within a narrow range (0.47–0.72 mg kg^{-1}). According to Pauletti and Motta (2017), these values are classified as medium to high, indicating adequate Cu availability across all treatments and the absence of Cu-related nutritional constraints during the ratoon cycle.

Soil Zn contents showed no significant differences among Ca–Mg–S sources ($p > 0.05$); however, within the control treatment, a significant difference between K sources was observed ($p \leq 0.05$). The phonolite source resulted in Zn contents (1.90 mg kg^{-1}) statistically higher than those obtained with clayey siltstone (0.53 mg kg^{-1}). Agronomically, this difference corresponds to a shift from the medium to the high Zn fertility class. Despite its statistical significance, this effect was restricted to the control treatment and did not reflect a consistent response to K source selection under Ca–Mg–S amendments.

Soil Mn contents were strongly influenced by Ca–Mg–S sources ($p \leq 0.05$). Control treatments exhibited the highest Mn values (18.48–18.88 mg kg^{-1}), statistically superior to all amended treatments and classified as high, a range associated with increased Mn availability under acidic conditions. The application of Ca–Mg–S sources significantly reduced Mn contents to values between 12.68 and 14.25 mg kg^{-1}, shifting Mn availability from the high to the medium fertility class. These reductions were consistent across K sources, indicating that Mn availability during the ratoon cycle was primarily regulated by Ca–Mg–S amendments rather than by K source selection.

Soil Fe contents were also significantly affected by Ca–Mg–S sources ($p \leq 0.05$). The control treatments presented the highest Fe contents (15.00–16.50 mg kg^{-1}), classified as high, whereas Ca–Mg–S amendments reduced Fe contents to values ranging from 7.25 to 11.75 mg kg^{-1}, corresponding predominantly to the medium fertility class. Despite these statistically significant reductions, Fe levels remained within adequate ranges for sugarcane nutrition, and no significant differences were detected between K sources within each Ca–Mg–S treatment.

Overall, the statistically significant effects of Ca–Mg–S sources during the ratoon cane cycle resulted in agronomically meaningful improvements in soil chemical status, particularly through the maintenance of medium to high pH and the reduction of excessive Mn and Fe availability. In contrast, statistically significant differences associated with K sources were limited, treatment-specific, and of minor agronomic relevance. These results indicate that the residual effects of Ca–Mg–S amendments persist into the ratoon cycle, contributing to sustained soil chemical balance without inducing micronutrient deficiencies in the surface layer.

Soil pH differed significantly among Ca–Mg–S sources ($p \leq 0.05$). Control treatments presented the lowest pH values (5.03–5.17), which were statistically inferior to treatments receiving rhythmite alone or in combination with limestone and classified as low to medium. The application of rhythmite, either alone or combined with limestone, significantly increased soil pH to values between 6.22 and 6.50, shifting the soil to the high pH class. Limestone applied alone or combined with gypsum or fidagran resulted in intermediate pH values (5.28–5.62), classified as medium, and did not differ statistically from the control in all cases, indicating a more limited liming effect at this depth.

Exchangeable Cu contents showed no significant differences among Ca–Mg–S sources ($p > 0.05$), remaining within a narrow range (1.30–1.58 mg kg^{-1}) and classified as high according to Pauletti and Motta (2017). However, within the limestone treatment, a significant difference between K sources was observed ($p \leq 0.05$), with clayey siltstone resulting in higher Cu concentrations than phonolite (1.58 vs. 1.30 mg kg^{-1}). Despite its statistical significance, this difference did not result in a change in Cu fertility class and is therefore considered agronomically marginal.

Soil Mn contents were strongly affected by Ca–Mg–S sources ($p \leq 0.05$). Control treatments exhibited the highest Mn values (11.75–16.40 mg kg^{-1}), classified as high, whereas Ca–Mg–S amendments significantly reduced Mn contents to values between 6.67 and 10.53 mg kg^{-1}, shifting Mn availability from the high to the medium fertility class. Within the rhythmite treatment, Mn contents differed significantly between K sources ($p \leq 0.05$), with phonolite resulting in higher Mn levels than clayey siltstone (9.68 vs. 6.78 mg kg^{-1}). Agronomically, both values remained within the medium class, indicating that this interaction, although statistically significant, has limited practical relevance.

Table 5
Mean soil pH and nutrient contents in the 0–20 cm layer as affected by treatments during the ratoon cane cycle.

Plots	Subplots	pH	Cu (mg kg^{-1})	Fe (mg kg^{-1})	Mn (mg kg^{-1})	Zn (mg kg^{-1})
Control	Clayey Siltstone	4.95 bA	0.72 aA	16.50 aA	18.88 aA	0.53 aB
Control	Phonolite	4.97 bA	0.55 aA	15.00 aA	18.48 aA	1.90 aA
Limestone	Clayey Siltstone	5.80 aA	0.57 aA	7.50 bA	12.68 bA	0.62 aA
Limestone	Phonolite	5.62 aA	0.62 aA	8.50 bA	12.78 bA	0.88 aA
Rhythmite	Clayey Siltstone	5.95 aA	0.50 aA	10.25 bA	13.97 bA	0.70 aA
Rhythmite	Phonolite	5.83 aA	0.55 aA	9.75 bA	13.62 bA	0.53 aA
Limestone + Rhythmite	Clayey Siltstone	6.17 aA	0.55 aA	7.25 bA	13.15 bA	0.58 aA
Limestone + Rhythmite	Phonolite	6.20 aA	0.55 aA	8.75 bA	14.12 bA	0.90 aA
Limestone + Gypsum	Clayey Siltstone	5.55 aA	0.65 aA	11.75 bA	14.25 bA	0.57 aA
Limestone + Gypsum	Phonolite	5.58 aA	0.47 aA	10.75 bA	14.00 bA	0.65 aA
Limestone + Fidagran	Clayey Siltstone	6.08 aA	0.62 aA	8.25 bA	13.80 bA	0.88 aA
Limestone + Fidagran	Phonolite	6.05 aA	0.52 aA	7.75 bA	13.60 bA	0.88 aA

Means followed by the same lowercase letter do not differ among Ca–Mg–S sources (main plots), while uppercase letters indicate differences among K sources within each Ca–Mg–S source (subplots), according to Tukey's test ($p \leq 0.05$).

Table 6
Mean soil pH and nutrient contents in the 20–40 cm layer as affected by treatments during the plant cane cycle.

Plots	Subplots	pH	Cu (mg kg^{-1})	Fe (mg kg^{-1})	Mn (mg kg^{-1})	Zn (mg kg^{-1})
Control	Clayey Siltstone	5.03 bA	1.48 aA	10.50 aA	16.40 aA	0.50 aA
Control	Phonolite	5.17 bA	1.45 aA	10.75 aA	11.75 aA	0.93 aA
Limestone	Clayey Siltstone	5.47 bA	1.58 aA	11.75 aA	10.53 bA	0.35 aA
Limestone	Phonolite	5.62 bA	1.30 aB	6.75 aA	8.22 bA	0.60 aA
Rhythmite	Clayey Siltstone	6.22 aA	1.43 aA	9.00 aA	6.78 bB	0.33 aA
Rhythmite	Phonolite	6.25 aA	1.42 aA	6.00 aA	9.68 bA	0.47 aA
Limestone + Rhythmite	Clayey Siltstone	6.50 aA	1.32 aA	8.00 aA	6.67 bA	0.45 aA
Limestone + Rhythmite	Phonolite	6.30 aA	1.35 aA	6.75 aA	7.00 bA	0.40 aA
Limestone + Gypsum	Clayey Siltstone	5.28 bA	1.48 aA	10.50 aA	9.10 bA	0.75 aA
Limestone + Gypsum	Phonolite	5.62 bA	1.45 aA	9.25 aA	7.75 bA	0.62 aA
Limestone + Fidagran	Clayey Siltstone	5.53 bA	1.30 aA	6.75 aA	9.97 bA	0.48 aA
Limestone + Fidagran	Phonolite	5.62 bA	1.40 aA	6.25 aA	7.52 bA	0.38 aA

Means followed by the same lowercase letter do not differ among Ca–Mg–S sources (main plots), while uppercase letters indicate differences among K sources within each Ca–Mg–S source (subplots), according to Tukey's test ($p \leq 0.05$).

Soil Fe contents did not differ significantly among Ca–Mg–S sources or between K sources ($p > 0.05$), with values ranging from 6.00 to 11.75 mg kg^{-1} and classified as medium to high. Similarly, soil Zn concentrations showed no significant differences among treatments ($p > 0.05$), remaining within a narrow range (0.33–0.93 mg kg^{-1}) and predominantly classified as medium, with no indication of Zn deficiency at this depth.

Overall, the statistically significant effects of Ca–Mg–S sources in the subsurface layer during the plant cane cycle were primarily associated with increases in soil pH and reductions in Mn availability, resulting in agronomically relevant shifts from high Mn availability to medium, non-restrictive levels. In contrast, statistically significant differences involving K sources were isolated and did not translate into meaningful changes in soil fertility classes, reinforcing the dominant role of Ca–Mg–S amendments in regulating subsurface soil chemical conditions.

During the ratoon cane cycle, soil chemical attributes in the 20–40 cm layer showed a significantly response to Ca–Mg–S sources only for soil pH, whereas K sources did not significantly affect any of the evaluated variables (Table 7).

Soil pH differed significantly among Ca–Mg–S sources ($p \leq 0.05$). The control treatments exhibited the lowest pH values, ranging from 4.83-4.92, and were statistically lower than all amended treatments. Limestone and limestone + gypsum resulted in intermediate pH values, ranging from 5.38 to 5.45, while the highest pH values were observed under rhythmite, limestone + rhythmite, and limestone + fidagran treatments, ranging from 5.78 to 6.25. These results indicate that Ca–Mg–S amendments increased soil pH in the subsurface layer during the ratoon cycle, with stronger responses associated with rhythmite-containing treatments and limestone + fidagran.

Exchangeable Cu contents were not significantly affected by either Ca–Mg–S sources or K sources ($p > 0.05$). Values ranged from 0.65 to 1.00 mg kg^{-1}, indicating that Cu availability remained relatively stable across treatments.

Soil Fe contents also showed no significant differences among Ca–Mg–S sources or between K sources ($p > 0.05$). Although Fe values varied numerically from 7.25 to 17.50 mg kg^{-1}, the absence of statistical differences indicates that the observed variation was not consistent enough to characterize a treatment effect.

Similarly, soil Mn contents were not significantly affected by Ca–Mg–S sources or K sources ($p > 0.05$). Values ranged from 8.05 to 15.25 mg kg^{-1}. Numerically, the lowest Mn contents were observed under rhythmite, limestone + rhythmite, and limestone + fidagran treatments, while the highest values occurred in the control treatments; however, these differences were not statistically significant.

Soil Zn contents did not differ significantly among treatments ($p > 0.05$), with values ranging from 0.25 to 0.67 mg kg^{-1}. No significant effect of K source was observed within any Ca–Mg–S treatment.

Overall, the results for the 20–40 cm layer during the ratoon cane cycle indicate that Ca–Mg–S amendments significantly improved subsurface soil pH, particularly when rhythmite or limestone + fidagran were applied. However, Cu, Fe, Mn, and Zn availability were not significantly altered by Ca–Mg–S sources or by K sources, suggesting that the main residual effect of the amendments at this depth was related to soil acidity correction rather than to consistent changes in micronutrient availability.

3.3. *Effect of the application of mining coproducts on plant attributes*

Leaf nutrient accumulation and stalk yield during the plant cane cycle were not significantly affected by Ca–Mg–S sources applied to the main plots or by K sources applied to the subplots (Table 8). Stalk yield values ranged from 99,182 to 128,119 kg ha^{-1}, with no statistically significant differences among treatments. Numerically, the highest stalk yield values were observed under the combined application of limestone and rhythmite, reaching 128119 kg ha^{-1} with the clayey siltstone source, which represents an increase of approximately 29% compared with the lowest yield observed in the control treatment with phonolite.

Copper accumulation in plant tissues remained statistically similar

Table 7
Mean soil pH and nutrient contents in the 20–40 cm layer as affected by treatments during the ratoon cane cycle.

Plots	Subplots	pH	Cu (mg kg^{-1})	Fe (mg kg^{-1})	Mn (mg kg^{-1})	Zn (mg kg^{-1})
Control	Clayey Siltstone	4.83 cA	0.90 aA	17.50 aA	15.25 aA	0.55 aA
Control	Phonolite	4.92 cA	0.98 aA	15.00 aA	13.25 aA	0.50 aA
Limestone	Clayey Siltstone	5.40 bA	0.68 aA	11.00 aA	10.52 aA	0.50 aA
Limestone	Phonolite	5.42 bA	0.80 aA	12.00 aA	10.75 aA	0.67 aA
Rhythmite	Clayey Siltstone	6.00 aA	1.00 aA	8.00 aA	8.07 aA	0.30 aA
Rhythmite	Phonolite	5.88 aA	0.70 aA	9.00 aA	8.90 aA	0.50 aA
Limestone + Rhythmite	Clayey Siltstone	6.00 aA	0.90 aA	8.75 aA	8.05 aA	0.30 aA
Limestone + Rhythmite	Phonolite	6.25 aA	0.77 aA	7.25 aA	9.15 aA	0.40 aA
Limestone + Gypsum	Clayey Siltstone	5.38 bA	0.93 aA	14.25 aA	11.65 aA	0.43 aA
Limestone + Gypsum	Phonolite	5.45 bA	0.68 aA	11.75 aA	12.72 aA	0.50 aA
Limestone + Fidagran	Clayey Siltstone	5.78 aA	0.77 aA	7.75 aA	8.50 aA	0.25 aA
Limestone + Fidagran	Phonolite	6.03 aA	0.65 aA	8.00 aA	9.18 aA	0.40 aA

Means followed by the same lowercase letter do not differ among Ca–Mg–S sources (main plots), while uppercase letters indicate differences among K sources within each Ca–Mg–S source (subplots), according to Tukey's test ($p \leq 0.05$).

across all treatments, ranging from 25.60 to 34.35 g ha^{-1}, while Zn accumulation showed no significant differences among treatments, remaining within 60.91 to 89.21 g ha^{-1}. Iron accumulation ranged from 217.24 to 430.22 g ha^{-1}, and Mn accumulation varied from 264.01 to 434.02 g ha^{-1}, with numerically higher values under limestone plus gypsum and rhythmite-based treatments. Despite the numerical variation observed — the highest Fe accumulation under limestone plus rhythmite with clayey siltstone was approximately 98% greater than the lowest value in the control, and the highest Mn accumulation under limestone plus gypsum was approximately 64% higher than the lowest value under limestone plus fidagran — none of these differences were statistically significant across Ca–Mg–S or K sources. Overall, leaf micronutrient accumulation and stalk yield during the plant cane cycle were not significantly altered by Ca–Mg–S or K sources, despite numerical trends suggesting greater nutrient accumulation and yield under combined Ca–Mg–S treatments.

Leaf nutrient accumulation and stalk yield during the ratoon cane cycle were not significantly affected by Ca–Mg–S sources applied to the main plots or by K sources applied to the subplots (Table 9). Stalk yield values ranged from 87,582 to 107,247 kg ha^{-1}, with no statistically significant differences among treatments. Numerically, the highest stalk yield value was observed under the rhythmite treatment with phonolite, which was approximately 22% higher than the lowest yield recorded in the control treatment with clayey siltstone.

Copper and Zn accumulation remained statistically similar across all treatments during the ratoon cycle, ranging from 25.78 to 31.32 g ha^{-1} and 61.70 to 84.24 g ha^{-1}, respectively. Iron accumulation ranged from 225.36 to 400.00 g ha^{-1}, with the highest values under the combined application of limestone and rhythmite with phonolite (approximately 77% greater than the lowest value in the control), and Mn accumulation ranged from 276.70 to 446.45 g ha^{-1}, with numerically higher values under rhythmite-based treatments. As in the plant cane cycle, none of these differences were statistically significant across Ca–Mg–S or K sources. Overall, these results confirm that leaf micronutrient accumulation and stalk yield were not significantly influenced by Ca–Mg–S or K sources across either crop cycle, indicating strong physiological buffering of micronutrient uptake in sugarcane regardless of the substantial soil chemical modifications induced by the amendments.

3.4. Integrated statistical analysis of soil and plant responses

The linear mixed-effects models revealed distinct responses of soil and plant variables to crop cycle, soil depth, and their interaction (Table 10). Soil pH was not significantly affected by crop cycle (plant vs. ratoon), soil depth (0–20 vs. 20–40 cm), or by the interaction between these factors, with p-values greater than 0.43 for all fixed effects.

In contrast, several soil micronutrients showed significant effects of crop cycle and soil depth. Soil Cu contents were significantly affected by both crop cycle and soil depth ($p < 0.001$ for both factors), whereas the interaction between cycle and depth was not significant ($p = 0.9123$). Similarly, soil Mn contents were significantly influenced by crop cycle ($p = 0.0005$) and soil depth ($p < 0.001$), with no significant interaction between factors.

Soil Fe contents were significantly affected by crop cycle ($p = 0.0015$), while soil depth and the interaction between crop cycle and depth were not significant ($p = 0.4729$ and 0.8253, respectively). Soil Zn contents were significantly influenced by crop cycle ($p = 0.0053$) and soil depth ($p < 0.001$), with no significant interaction detected ($p = 0.1112$).

Stalk yield was significantly affected by crop cycle ($p < 0.001$), indicating differences in productivity between plant cane and ratoon cane. In contrast, leaf nutrient accumulation variables, including Cu, Fe, Mn, and Zn accumulation, were not significantly influenced by crop cycle, with p-values ranging from 0.8323 to 0.9914.

Overall, the mixed-model analysis indicates that soil micronutrient contents were primarily influenced by crop cycle and soil depth, whereas leaf nutrient accumulation was stable across crop cycles, and no significant interactions between crop cycle and soil depth were detected for any of the evaluated variables.

The principal component analysis (PCA) of soil chemical attributes indicated that the first two components explained 64.6% of the total variance, with PC1 accounting for 42.9% and PC2 for 21.7% (Fig. 4a). The first principal component was primarily associated with soil pH, which showed strong positive loadings, whereas extractable Fe and Mn exhibited negative loadings along this axis. Accordingly, samples were mainly separated along PC1 according to gradients of soil acidity and Fe–Mn availability, with Ca–Mg–S–amended treatments positioned toward higher PC1 values and the control treatments toward lower PC1 values.

The second principal component of the soil PCA was mainly associated with extractable Cu, which showed the strongest loading along PC2. Zn contributed moderately to both PC1 and PC2, whereas Mn showed a stronger association with PC1. Partial separation between crop cycles was observed along PC2, with ratoon samples more frequently positioned in the negative region of this axis.

In contrast, the PCA of plant tissue variables showed a different

Table 8
Mean leaf accumulation of Cu, Fe, Mn, and Zn and stalk yield in sugarcane during the plant cane cycle, grouped by treatment.

Plots	Subplots	Stalk yield (kg ha^{-1})	Cu accumulation (g ha^{-1})	Fe accumulation (g ha^{-1})	Mn accumulation (g ha^{-1})	Zn accumulation (g ha^{-1})
Control	Clayey Siltstone	107933.33 aA	28.42 aA	249.26 abA	403.51 aA	66.39 aA
Control	Phonolite	99181.67 8 aA	25.60 aA	217.24 bA	351.07 aA	60.91 aA
Limestone	Clayey Siltstone	119902.22 aA	28.74 aA	336.58 abA	391.25 aA	71.25 aA
Limestone	Phonolite	113146.67 aA	27.10 aA	282.21 abA	351.40 aA	69.24 aA
Rhythmite	Clayey Siltstone	113883.33 aA	28.33 aA	311.68 abA	372.21 aA	77.90 aA
Rhythmite	Phonolite	114561.11 aA	28.52 aA	323.78 abA	406.18 aA	74.53 aA
Limestone + Rhythmite	Clayey Siltstone	128118.89 aA	34.35 aA	430.22 aA	363.30 aA	89.21 aA
Limestone + Rhythmite	Phonolite	111483.33 aA	30.07 aA	361.38 abA	321.55 aA	75.70 aA
Limestone + Gypsum	Clayey Siltstone	125807.78 aA	31.68 aA	332.15 abA	434.02 aA	88.79 aA
Limestone + Gypsum	Phonolite	111200.56 aA	27.86 aA	308.72 abA	360.44 aA	74.58 aA
Limestone + Fidagran	Clayey Siltstone	110217.22 aA	27.33 aA	245.26 bA	264.01 aA	74.38 aA
Limestone + Fidagran	Phonolite	117483.33 aA	29.50 aA	260.13 abA	298.52 aA	79.60 aA

Means followed by the same lowercase letter do not differ among Ca–Mg–S sources (main plots), while uppercase letters indicate differences among K sources within each Ca–Mg–S source (subplots), according to Tukey's test ($p \leq 0.05$).

Table 9
Mean leaf accumulation of Cu, Fe, Mn, and Zn and stalk yield in sugarcane during the ratoon cane cycle, grouped by treatment.

Plots	Subplots	Stalk yield (kg ha^{-1})	Cu accumulation (g ha^{-1})	Fe accumulation (g ha^{-1})	Mn accumulation (g ha^{-1})	Zn accumulation (g ha^{-1})
Control	Clayey Siltstone	87582.22 aA	26.63 aA	235.17 cA	382.23 aA	61.70 aA
Control	Phonolite	87704.33 aA	26.65 aA	225.36 cA	368.99 aA	63.02 aA
Limestone	Clayey Siltstone	91862.78 aA	25.78 aA	302.13 abcA	355.95 aA	63.08 aA
Limestone	Phonolite	97648.89 aA	27.40 aA	285.28 abcA	355.38 aA	70.15 aA
Rhythmite	Clayey Siltstone	98166.67 aA	28.21 aA	321.40 abcA	376.90 aA	78.72 aA
Rhythmite	Phonolite	107246.67 aA	31.29 aA	333.36 abcA	446.45 aA	81.95 aA
Limestone + Rhythmite	Clayey Siltstone	98551.11 aA	30.93 aA	369.75 abA	330.75 aA	79.60 aA
Limestone + Rhythmite	Phonolite	99247.78 aA	31.32 aA	400.00 aA	335.34 aA	78.97 aA
Limestone + Gypsum	Clayey Siltstone	92816.67 aA	27.54 aA	296.37 abcA	372.34 aA	77.62 aA
Limestone + Gypsum	Phonolite	106300.00 aA	31.17 aA	322.07 abcA	404.14 aA	84.24 aA
Limestone + Fidagran	Clayey Siltstone	97671.11 aA	28.15 aA	246.93 bcA	276.70 aA	77.57 aA
Limestone + Fidagran	Phonolite	104525.56 aA	30.60 aA	284.44 abcA	314.04 aA	82.46 aA

Means followed by the same lowercase letter do not differ among Ca–Mg–S sources (main plots), while uppercase letters indicate differences among K sources within each Ca–Mg–S source (subplots), according to Tukey's test ($p \leq 0.05$).

Table 10
Mixed linear models for soil and plant variables.

Variable	P–cycle	P – depth	P – interaction cycle × depth	Converged
pH	0.9676^{ns}	0.9514^{ns}	0.4382^{ns}	Yes
Cu	0**	0**	0.9123^{ns}	Yes
Fe	0.0015**	0.4729^{ns}	0.8253^{ns}	Yes
Mn	0.0005**	0**	0.2392^{ns}	Yes
Zn	0.0053**	0**	0.1112^{ns}	Yes
Stalk yield (kg ha^{-1})	0**	–	–	Yes
Cu accumulation (g ha^{-1})	0.8658^{ns}	–	–	Yes
Fe accumulation (g ha^{-1})	0.8323^{ns}	–	–	Yes
Mn accumulation (g ha^{-1})	0.9914^{ns}	–	–	Yes
Zn accumulation (g ha^{-1})	0.9229	–	–	Yes

P-values refer to fixed effects of crop cycle (plant vs. ratoon), soil depth (0–20 vs. 20–40 cm), and their interaction.

multivariate structure (Fig. 4b). The first two principal components explained 79.5% of the total variance, with PC1 accounting for 59.5% and PC2 for 20.0%. The first principal component was mainly associated with stalk yield and the accumulation of Fe, Zn, and Mn in plant tissues, as indicated by the direction and length of the vectors. Samples were primarily distributed along PC1 according to variation in these variables, with higher PC1 scores corresponding to greater yield and micronutrient accumulation.

The second principal component of the plant PCA was predominantly associated with Cu accumulation, which showed the highest loading along PC2. Compared with the soil PCA, the plant PCA exhibited a more compact clustering of samples and substantial overlap among treatments and crop cycles, indicating limited multivariate differentiation in plant responses.

Overall, the comparison between soil and plant PCAs indicates that soil chemical attributes exhibited stronger multivariate separation among treatments, driven mainly by pH and Fe–Mn availability, whereas plant tissue variables and yield showed reduced dispersion and weaker treatment discrimination, despite the pronounced variability observed in soil chemical conditions. From a management standpoint, this decoupling suggests that soil chemical indicators are more sensitive

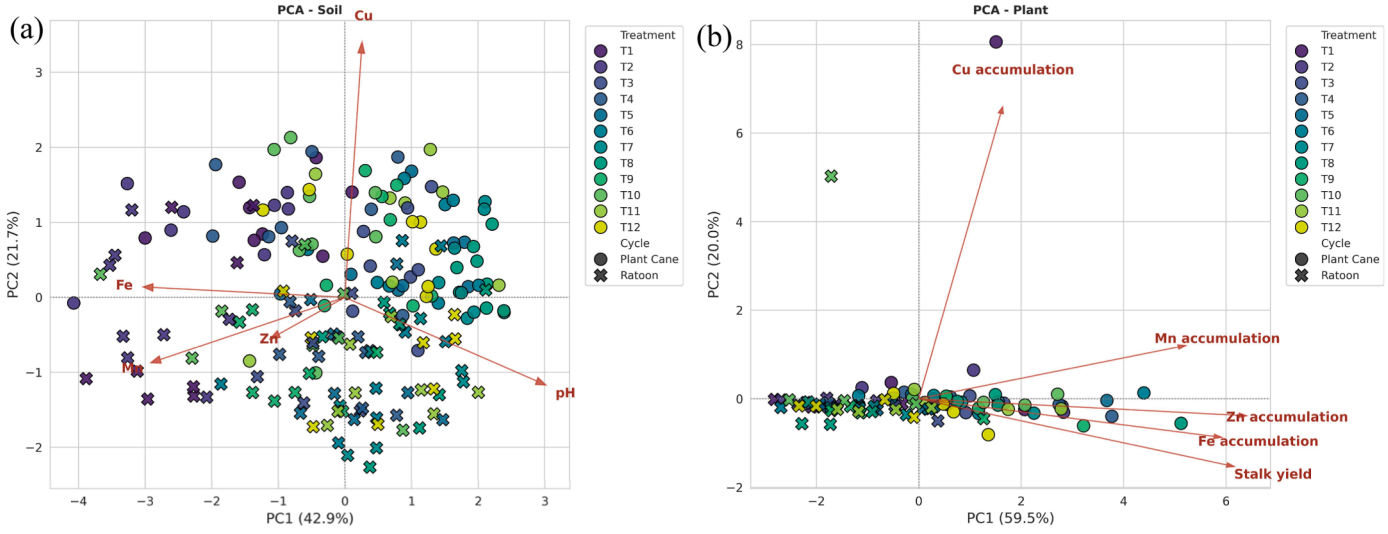

Fig. 4. Principal Component Analysis (PCA) biplot illustrating the multivariate relationships among soil chemical attributes (a) and plant (b) responses under different treatments, soil depths, and crop cycles.

early-response diagnostics for amendment efficacy, whereas plant-based metrics may require longer time horizons or more limiting baseline conditions to reflect treatment effects.

The heatmap of Pearson correlation coefficients illustrates the relationships among soil chemical attributes, leaf micronutrient accumulation, and stalk yield (Fig. 5). Correlation coefficients ranged from −0.65 to 0.83, indicating weak to strong linear associations among variables.

Soil pH showed a moderate to strong negative correlation with extractable Fe ($r = -0.65$) and a moderate negative correlation with extractable Mn ($r = -0.50$). In contrast, correlations between soil pH and Cu ($r = -0.14$) or Zn ($r = -0.08$) were weak. Soil pH exhibited only a weak positive correlation with stalk yield ($r = 0.18$).

Among soil micronutrients, extractable Fe and Mn were moderately positively correlated ($r = 0.49$), whereas correlations between Mn and Zn ($r = 0.28$) and between Fe and Zn ($r = 0.05$) were weak. Soil Cu showed weak correlations with Fe ($r = -0.09$), Mn ($r = -0.17$), and Zn ($r = 0.03$).

Stalk yield was moderately to strongly positively correlated with leaf micronutrient accumulation, particularly with Zn accumulation ($r = 0.83$) and Fe accumulation ($r = 0.73$), and showed a moderate positive correlation with Mn accumulation ($r = 0.48$). Correlations between stalk yield and soil micronutrient concentrations were generally weak to moderate, ranging from −0.36 (Fe) to 0.38 (Cu).

Correlations between soil extractable micronutrients and their corresponding leaf accumulation were generally weak. Soil Cu showed a weak correlation with Cu accumulation ($r = 0.22$), soil Fe with Fe accumulation ($r = -0.26$), soil Mn with Mn accumulation ($r = -0.07$), and soil Zn with Zn accumulation ($r = 0.20$).

Overall, the correlation matrix indicates that soil pH was primarily associated with extractable Fe and Mn, whereas stalk yield was more strongly associated with leaf micronutrient accumulation than with soil chemical attributes.

4. Discussion

4.1. Mineralogical characteristics of mining coproduct and implications for nutrient dynamics

The contrasting effects observed among coproducts are primarily governed by their mineralogical composition and associated reactivity within the soil environment. Limestone, rhythmite, gypsum-based materials, and fidagran differ substantially in dominant mineral phases, crystallinity, solubility, and acid-neutralizing capacity, which collectively determine their dissolution kinetics and interaction with the soil matrix. Carbonate-rich materials, such as limestone and rhythmite (containing calcite and dolomite; Fig. 3), increase soil pH through proton consumption and release of Ca^{2+} and Mg^{2+}, whereas gypsum-based sources supply Ca and S without directly neutralizing soil acidity.

Among the evaluated materials, rhythmite—applied alone or in combination with limestone—exhibited the greatest capacity to increase

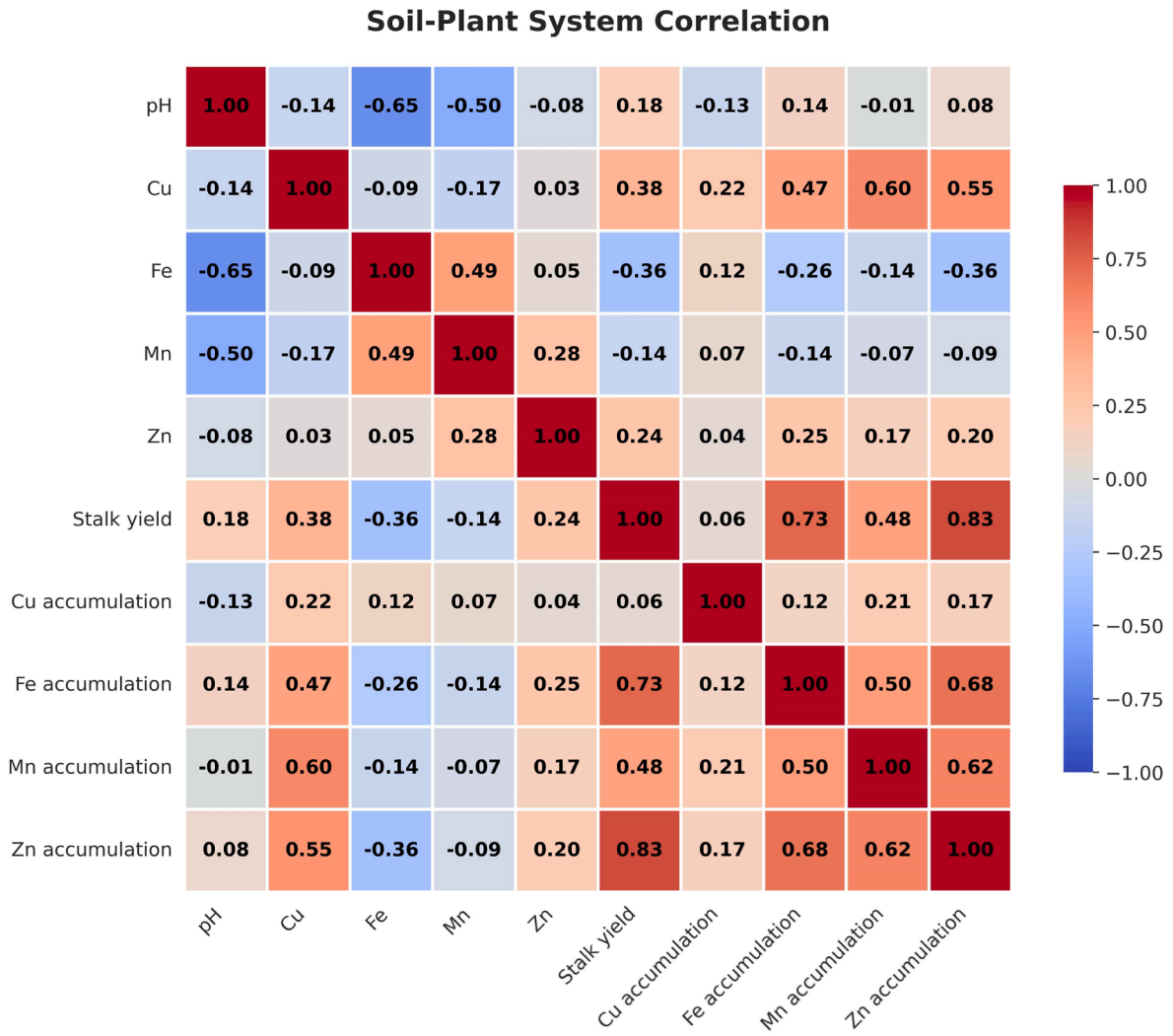

Fig. 5. Heatmap of Pearson correlation coefficients among soil chemical attributes, leaf micronutrient accumulation, and stalk yield across inputs source treatments, soil depths, and crop cycles.

soil pH, with effects extending from the surface into the subsurface and persisting across crop cycles. This behavior is attributed to the presence of reactive carbonate phases (calcite and dolomite) combined with finer particle size and higher specific surface area, which enhance dissolution rates and promote greater contact with soil colloids. The importance of particle size is well-established: particles <250 μm (60-mesh) exhibit 100% effectiveness in neutralizing soil acidity, whereas particles >2000 μm (10-mesh) have negligible short-term reactivity (Liu et al., 2010; Rauch and White, 1977; Yasuda et al., 2013). Our rhythmite, with 70% < 0.84 mm and 50% < 0.30 mm, falls within the highly reactive size range, explaining its superior performance relative to coarser conventional limestone applications.

Additionally, calcite reacts approximately twice as fast as dolomite due to differential dissolution kinetics (Yasuda et al., 2013). However, dolomite-containing materials like rhythmite can achieve sustained pH increases due to continued Mg^{2+} release over extended periods, consistent with observations that dolomitic limestones maintain residual neutralizing capacity longer than calcitic sources (du Toit et al., 2024; Jones and Mallarino, 2018). Recent studies confirm that limes with high Mg content show enhanced acid sensitivity and reactivity (Bassioni et al., 2021), supporting our findings of rhythmite's superior effectiveness.

The mineralogical control of soil acidity also exerted decisive influence on micronutrient dynamics. Increases in soil pH induced by carbonate-rich sources consistently reduced extractable Mn and, to a lesser extent, Fe contents, shifting these elements from high to medium fertility classes across depths and crop cycles. This response reflects the strong pH dependence of Mn and Fe solubility, driven by oxidation–precipitation reactions and increased sorption onto Fe and Al oxides under less acidic conditions (Goulding, 2016; Holland et al., 2018). Manganese is particularly sensitive to pH changes: below pH 5.2, Mn solubility increases exponentially, reaching potentially phytotoxic levels in acidic soils. The pH-mediated reduction of Mn from 15 to 18 mg kg^{-1} (control) to 8–14 mg kg^{-1} (amended treatments) aligns with documented thresholds for Mn toxicity mitigation while maintaining adequate plant nutrition.

In contrast, Cu and Zn concentrations exhibited limited sensitivity to Ca–Mg–S sources, with most treatments maintaining these elements within medium to high fertility classes regardless of pH changes. This stability suggests that, under the studied conditions, sorption mechanisms controlling Cu and Zn availability were buffered by organic matter and clay mineral interactions or by micronutrient inputs from the coproducts themselves (Table 1: 11–70 mg kg^{-1} total Zn; 4.8–25.3 mg kg^{-1} total Cu). Similar buffering has been reported for sandy soils with low clay content, where Zn availability remains stable despite pH increases when alternative amendments supply residual micronutrients (Barreto et al., 2024; Richardson, 2024).

Overall, the results demonstrate that mineralogical characteristics of Ca–Mg–S sources govern not only liming efficiency but also the magnitude, persistence, and depth of their effects on soil micronutrient dynamics. Carbonate-rich materials, particularly rhythmite-based treatments, promoted a more balanced soil chemical environment by simultaneously correcting acidity and regulating redox-sensitive micronutrients. These findings highlight the importance of considering mineralogical composition and particle size distribution, rather than solely nutrient content, when selecting Ca–Mg–S sources for sustainable soil fertility management in tropical agroecosystems.

4.2. Soil chemical responses to mining coproducts across depths and crop cycles

The application of Ca–Mg–S sources exerted consistent and agronomically relevant effects on soil chemical attributes, with soil pH and Mn availability emerging as the most responsive variables.

Statistically significant pH increases occurred in both surface (0–20 cm) and subsurface (20–40 cm) layers, with treatments combining limestone and rhythmite promoting the highest values (6.4–6.5). This cumulative liming effect persisted from the plant cane to ratoon cycle, shifting fertility classes from low to medium or high. These responses align with global meta-analyses showing that liming positively influences soil pH and crop yields across diverse soil types (Enesi et al., 2023), with typical pH increases of 0.93–1.64 units within 9 months in tropical sugarcane systems (López-Hernández et al., 2013).

However, rhythmite-based treatments achieved greater subsurface pH increases (ΔpH = 1.0–1.5 at 20–40 cm) compared to conventional calcitic limestone. This enhanced downward mobility reflects the finer particle size distribution (70% < 0.84 mm), higher reactivity, and mineralogical composition (reactive dolomite and calcite; Fig. 3a) of mining coproducts (Enesi et al., 2023; Manning and Theodoro, 2020; Rodrigues et al., 2024a). The persistence of pH effects into the ratoon cycle is consistent with reports of conventional calcitic limestone maintaining residual neutralizing capacity for 2–4 years in tropical sugarcane systems (Ejigu et al., 2023), suggesting that carbonate-rich mining coproducts, particularly those with finer particle size and dolomitic composition, may offer comparable or extended longevity relative to standard agricultural lime.

Control treatments with low pH exhibited high Mn availability (15–18 mg kg^{-1}), whereas Ca–Mg–S amendments significantly reduced Mn concentrations to 8–14 mg kg^{-1} across depths and cycles, mitigating toxicity risk without inducing deficiency. This pH-mediated Mn reduction is well-documented in tropical soils, where lime application prevents Mn and Al solubility, particularly below pH 5.2 where phytotoxic levels occur in weathered Ultisols and Oxisols (Goulding, 2016; Holland et al., 2018).

Surface layers showed greater Mn reduction (40–60%) than subsurface layers (20–35%), consistent with pH stratification patterns. However, unlike conventional lime where subsurface Mn remains largely unchanged, rhythmite treatments reduced Mn even at 20–40 cm depth, suggesting that optimized particle size and reactive carbonate minerals facilitate greater cation mobility throughout the root zone. These reductions occurred without compromising plant Mn nutrition (section 4.4), as sugarcane is considered a Mn-tolerant crop (Zambrosi et al., 2016).

In contrast, Fe and Zn availability exhibited greater resilience to amendment-induced changes. Zn remained stable despite pH increases of up to 1.5 units, differing from expectations where liming induces micronutrient deficiencies through precipitation and increased sorption (Wenyika et al., 2025). This stability is consistent with the buffering mechanisms discussed in section 4.1, and Fe stability likely reflects redox buffering by iron oxides typical of weathered Brazilian soils, where dissolution is controlled primarily by redox potential rather than pH within the 5.0–6.5 range (Nishimoto et al., 2025).

Significant main effects of crop cycle and soil depth were detected for Cu, Mn, Fe, and Zn, reflecting dynamic micronutrient availability in sugarcane systems. However, the absence of significant cycle × depth interactions indicates that Ca–Mg–S effects remained consistent across soil layers and time, representing sustained modifications. This spatial-temporal stability contrasts with annual cropping systems where amendment effects dissipate within one season (Larkin, 2020), but aligns with long-term perennial crop trials where residual liming effects persist for 3–5 years (Enesi et al., 2023; Wenyika et al., 2025).

Overall, Ca–Mg–S mining coproducts improved soil chemical quality primarily through acidity correction and Mn regulation, with effects persisting across depths and cycles. The superior performance of rhythmite-based treatments in subsurface pH modification and Mn reduction represents a notable advancement for acidic tropical soils, aligning with growing recognition of rock powders as sustainable amendments supplying multiple nutrients while improving soil chemical balance (Manning and Theodoro, 2020; Rodrigues et al., 2021a; van Straaten, 2007).

4.3. Plant nutrient accumulation and yield responses

Despite pronounced and statistically consistent effects of Ca–Mg–S

sources on soil chemical attributes, plant responses were comparatively stable across treatments in both crop cycles. Stalk yield did not differ significantly among Ca–Mg–S or K sources, ranging from 88 to 128 Mg ha^{-1}, indicating that sugarcane productivity was not directly constrained by the variations in soil pH and micronutrient availability observed. These yield levels remained within commercially acceptable ranges, underscoring sugarcane's high adaptive capacity to spatial and temporal heterogeneity in soil fertility.

The absence of significant yield responses contrasts with field studies where liming increased sugarcane productivity by 15–40% in highly acidic soils (de Campos et al., 2022; Yuan et al., 2025), but aligns with reports where lime application failed to improve yields compared to unlimed controls (Besen et al., 2021; Enesi et al., 2023). This pattern reflects a fundamental agronomic principle: yield responses to amendments are most pronounced when baseline fertility limits crop performance.

In our Arenosol, despite low pH (4.95–5.07) in control treatments, the absence of aluminum toxicity (0.05 $cmol_c\ dm^{-3}$) and adequate base saturation (40%) likely maintained sufficient chemical conditions to support commercial growth. This interpretation is supported by meta-analytical findings showing that liming effects on crop yield are strongest when soil pH < 4.5 and exchangeable Al > 1.0 $cmol_c\ dm^{-3}$ (Wenyika et al., 2025), conditions not present in our experimental site. The yield stability across lime rates parallels observations in Brazilian sugarcane systems where excessive lime application improved soil pH without proportional yield increases (de Campos et al., 2022), suggesting diminishing agronomic returns beyond threshold acidity correction levels.

Leaf micronutrient accumulation exhibited limited sensitivity to Ca–Mg–S and K sources. The accumulation of Cu, Zn, Fe, and Mn in diagnostic leaves did not differ significantly among treatments, even with substantial differences in soil micronutrient availability (Mn: 8–18 mg kg^{-1}; Fe: 5–17 mg kg^{-1}). This decoupling reflects strong physiological regulation of micronutrient absorption in sugarcane, enabling maintenance of stable tissue concentrations across wide-ranging soil chemical conditions.

Plants have evolved highly specialized networks to optimize micronutrient uptake, distribution, and allocation to metalloproteins, particularly for transition metals with narrow optimal concentration ranges (Bouain et al., 2014; Saenchai et al., 2016). Multiple regulatory mechanisms operate simultaneously, including high-affinity transport systems, efflux transporters, intracellular chelation, and systemic signaling coordinating uptake at the whole-plant level (Chaiwong et al., 2020). For manganese specifically, despite potentially toxic soil levels (15–18 mg kg^{-1}) in control treatments, plant tissue Mn remained within adequate ranges (264–446 g ha^{-1}), as sugarcane—classified as Mn-tolerant—possesses effective regulatory mechanisms including apoplastic barriers, vacuolar sequestration, and preferential allocation to older leaves (Zambrosi et al., 2016).

The weak correlations between soil extractable micronutrients and leaf accumulation ($r = -0.26$ to 0.22; Fig. 5) further support this physiological buffering. Such decoupling has been extensively reported for Fe and Zn homeostasis, where cross-talk between nutrient signaling pathways maintains adequate tissue concentrations despite fluctuating soil availability (Belgaroui et al., 2022).

Additionally, sugarcane's extensive root system likely buffered short-term or surface-layer soil variations. Sugarcane roots extend beyond 2 m depth, with active roots concentrated in the 0–60 cm layer (Cruz et al., 2021), allowing access to residual nutrient pools beyond the 0–20 cm sampling depth and dampening effects of surface-applied amendments. High root plasticity enables preferential biomass allocation toward nutrient-rich patches (Lak et al., 2020), while residual nutrient pools, biological nitrogen fixation, and nutrient recycling from trash blankets contribute to stable nutritional status under variable amendment regimes (Iqbal et al., 2025).

Together, these results suggest that under adequate baseline fertility, Ca–Mg–S sources primarily enhance soil environment and reduce risks associated with acidity and micronutrient imbalance, rather than directly increasing short-term yield or tissue nutrient concentrations. This preventive, rather than corrective, role is particularly relevant for long-term soil fertility management in perennial cropping systems.

Future research should evaluate whether the documented soil chemical improvements translate to yield benefits under more limiting fertility conditions, such as in ratoon cycles beyond the second year, under water stress, or in soils with higher aluminum saturation. Long-term experiments (>5 years) are needed to assess cumulative effects of mining coproducts on soil fertility dynamics, ratoon longevity, and economic returns relative to conventional lime applications.

4.4. Integration of soil and plant responses

The integrated analysis reveals clear decoupling between soil chemical modification and short-term crop performance. Although Ca–Mg–S sources promoted substantial changes in soil pH and Mn availability, these improvements did not translate into proportional differences in plant micronutrient accumulation or stalk yield. This pattern was consistently supported by univariate, mixed-effects, and multivariate approaches, indicating that soil chemical modifications alleviated potential constraints without exceeding physiological thresholds required to elicit measurable plant performance gains within the study duration.

Principal component analysis reinforced this decoupling. Soil variables showed strong treatment separation along PC1 (42.9% of total variance), driven primarily by pH and Fe–Mn availability gradients, with Ca–Mg–S-amended treatments clearly displaced from control treatments. In contrast, plant tissue variables exhibited substantial overlap among treatments and crop cycles in their respective PCA space, despite PC1 capturing 59.5% of plant variance — a high proportion reflecting dominant co-variation among yield and micronutrient accumulation rather than treatment discrimination. This contrasting multivariate structure — where soil attributes responded sensitively to Ca–Mg–S sources while plant responses remained stable — is consistent with observations in other soil quality assessment studies using PCA to differentiate management effects (Abdel-Fattah et al., 2021; Emami et al., 2024), and aligns with long-term fertility experiments in which soil chemical indicators discriminated among treatments more effectively than plant-based metrics under non-limiting baseline fertility (Kazmierczak et al., 2020; Marinari et al., 2006).

Correlation analyses further support this interpretation. Strong associations existed among soil variables (pH vs. Fe: $r = -0.65$; pH vs. Mn: $r = -0.50$), but weak correlations connected soil chemistry to plant responses (soil Mn vs. plant Mn: $r = -0.07$; soil Fe vs. plant Fe: $r = -0.26$). This contrasts with expectations under nutrient-limiting conditions where soil-plant correlations typically strengthen (Chen et al., 2025; Fuentes et al., 2009). The pronounced soil Mn reduction under rhythmite treatments, while agronomically relevant for toxicity prevention, did not affect plant Mn accumulation, underscoring the importance of interpreting soil indicators within the context of physiological regulation rather than as direct predictors of plant status (Huang et al., 2016; Silva et al., 2024; Zambrosi et al., 2016).

The stability of Fe and Zn in plant tissues despite significant soil variations reflects buffering by soil mineral phases, micronutrient mobility constraints, and root-mediated uptake regulation. In sugarcane systems with deep root architecture and prolonged growth cycles, nutrient acquisition integrates conditions across depth and time, dampening localized or short-term soil chemical changes (Cruz et al., 2021; Lak et al., 2020).

Collectively, these results indicate that Ca–Mg–S sources primarily enhance soil chemical resilience and stability rather than drive immediate yield gains. From a management perspective, this reinforces the value of mining coproducts as preventive, sustainability-oriented strategies that maintain favorable soil conditions and reduce micronutrient imbalance risks over successive sugarcane cycles (Manning, 2018; Manning and Theodoro, 2020; Skov et al., 2024). This preventive

function aligns with soil quality frameworks emphasizing long-term maintenance of soil functions rather than short-term productivity maximization (Emami et al., 2024; Hannam et al., 2025; Richardson, 2024). However, the lack of yield responses suggests these improvements operated within non-limiting ranges, consistent with observations that soil fertility improvements do not always translate to immediate productivity gains when baseline conditions are adequate (Omara-Ojungu and Lukac, 2025).

4.5. Implications for soil fertility and management of sugarcane systems

These findings have direct implications for soil fertility management in tropical sugarcane production, where acidic soils and heterogeneous micronutrient availability constrain long-term productivity. The consistent increases in soil pH and concomitant reductions in Mn availability promoted by Ca–Mg–S amendments demonstrate their effectiveness in alleviating key chemical constraints that compromise soil functionality over time.

From a management perspective, the limited plant response emphasizes that the primary benefit of Ca–Mg–S amendments lies in sustaining favorable soil chemical conditions rather than generating immediate productivity gains. This preventive function aligns with integrated soil fertility management (ISFM) principles, which emphasize strategic combinations of mineral inputs and amendments to enhance nutrient use efficiency and sustain soil productivity over time (Saliu and Shehu, 2012). In perennial crops like sugarcane, where yield integrates soil conditions across depth and time, amendments should be viewed as strategic investments in system resilience aimed at preventing nutrient imbalances and maintaining optimal rooting environments across successive ratoon cycles (Borges et al., 2020; Cruz et al., 2021; de Campos et al., 2022; Zambrosi et al., 2016).

The minimal influence of K source selection on soil and plant responses indicates that, under adequate K supply, Ca–Mg–S material selection is prioritized over K source choice. This suggests that fertilizer strategies should prioritize acidity correction and Mn regulation while integrating K fertilization within broader, site-specific nutrient management frameworks (Huang et al., 2016; Silva et al., 2024). This approach is consistent with precision agriculture applications in sugarcane, where variable-rate lime and nutrient applications improve soil fertility distribution while maintaining stable yields and delivering economic benefits through reduced input costs (Pierpaoli et al., 2013; Srbinovska et al., 2015).

The valorization of mining coproducts as soil amendments supports circular economy principles, reducing reliance on conventional limestone quarrying while closing resource loops in agricultural systems (Manning, 2018; Manning and Theodoro, 2020; Richardson, 2024). Brazilian experience with soil remineralization demonstrates that legislative frameworks can facilitate integration of mining residues into agricultural nutrient management, with potential co-benefits for carbon sequestration and reduced environmental footprint (Khan, 2025; Martins et al., 2015; Ramos et al., 2015).

Overall, the integrated soil–plant responses support adoption of Ca–Mg–S mining coproducts as central components of sustainable soil fertility management in sugarcane systems. By improving soil chemical balance without inducing micronutrient deficiencies or compromising productivity, these amendments contribute to long-term stability and efficiency of sugarcane production under tropical conditions. Future research should evaluate economic feasibility, environmental life-cycle impacts, and long-term (>5 years) residual effects on soil fertility and ratoon longevity at regional scales.

5. Conclusion

Limestone mining coproducts applied as Ca–Mg–S sources promoted consistent and agronomically meaningful improvements in soil chemical quality, particularly through pH increases of up to 1.5 units and reductions in extractable Mn of 40–60% across depths and crop cycles. Carbonate-rich materials — especially rhythmite applied alone or combined with limestone — achieved the greatest and most persistent effects, reflecting the determinant role of mineralogical composition and particle size in governing dissolution kinetics and soil chemical modification in tropical Arenosols.

Linear mixed-effects models confirmed that soil micronutrient dynamics were primarily structured by soil depth and crop cycle, with no significant cycle × depth interactions. Leaf micronutrient accumulation and stalk yield — ranging from 88 to 128 Mg ha^{-1} across cycles — remained stable regardless of treatment, reflecting strong physiological buffering of nutrient uptake in sugarcane under heterogeneous soil chemical conditions.

The absence of short-term yield response does not indicate amendment inefficacy. Under moderate baseline fertility, these materials operated preventively — maintaining pH within optimal ranges and suppressing Mn availability before phytotoxic thresholds are reached — rather than correctively. In perennial systems such as sugarcane, this distinction is agronomically critical, as the value of acidity management accumulates across successive ratoon cycles over time scales that exceed typical experimental windows. Potassium source selection exerted no consistent influence on any response variable, confirming that Ca–Mg–S material choice is the dominant management lever under adequate K supply.

Collectively, these findings support the adoption of limestone mining coproducts as sustainable multinutrient amendments that improve soil chemical balance and reduce acidity- and Mn-related risks without compromising crop productivity, aligned with circular economy principles through the valorization of mining-derived materials. Future research should assess long-term cumulative effects (≥5 years) on ratoon longevity and soil carbon dynamics, and evaluate yield responses under more limiting conditions such as higher aluminium saturation or water deficit.

Funding

This study was funded by Coordenação de Aperfeiçoamento de Pessoal de Nível Superior (grant number: 88882.344504/2019e01).

CRediT authorship contribution statement

Marlon Rodrigues: Writing – original draft, Formal analysis. **Carlos Augusto Posser Silveira:** Supervision, Investigation, Formal analysis. **Everson Cezar:** Writing – review & editing, Methodology. **Glaucio Leboso Alemparte Abrantes dos Santos:** Writing – original draft, Data curation. **Leticia Romagna:** Software, Methodology. **Marcos Rafael Nanni:** Supervision, Conceptualization.

Declaration of the use of AI assisted technologies

During the preparation of this work, the author(s) used ChatGPT for paraphrasing and checking grammar. After using this tool/service, the author(s) reviewed and edited the content as needed and take(s) full responsibility for the content of the published article

Declaration of competing interest

The authors declare that they have no known competing financial interests or personal relationships that could have appeared to influence the work reported in this paper.

Acknowledgments

The authors would like to thank Calcário Diamante for providing the material evaluated in this study.

Appendix

Table A1
Summary of soil fertility class shifts for pH and extractable Mn as affected by Ca–Mg–S source treatments, across soil depths (0–20 cm and 20–40 cm) and crop cycles (plant cane and ratoon cane), classified according to Pauletti and Motta (2017).

Treatment	Soil pH								Extractable Mn (mg kg^{-1})							
	0–20 cm				20–40 cm				0–20 cm				20–40 cm			
	Plant cane value	Class	Ratoon value	Class	Plant cane value	Class	Ratoon value	Class	Plant cane value	Class	Ratoon value	Class	Plant cane value	Class	Ratoon value	Class
Control	4.95–5.07	Low	4.95–4.97	Low	5.03–5.17	Low	4.83–4.92	Low	15.22–18.32	Low-Medium	18.48–18.88	Medium	11.75–16.40	Low-Medium	13.25–15.25	Low
Limestone	5.38–5.85	Medium-High	5.62–5.80	High	5.47–5.62	Medium-High	5.40–5.42	Medium	10.88–13.48	Low	12.68–12.78	Low	8.22–10.53	Low	10.52–10.75	Low
Rhythmite	5.85–6.05	High	5.83–5.95	High	6.22–6.25	High	5.88–6.00	High	11.85–12.73	Low	13.62–13.97	Low	6.78–9.68	Low	8.07–8.90	Low
Limestone + Rhythmite	6.40–6.47	High	6.17–6.20	High	6.30–6.50	High	6.00–6.25	High	8.38–8.70	Low	13.15–14.12	Low	6.67–7.00	Low	8.05–9.15	Low
Limestone + Gypsum	5.42–5.88	Medium-High	5.55–5.58	Medium-High	5.28–5.62	Medium-High	5.38–5.45	Medium	12.18–12.75	Low	14.00–14.25	Low	7.75–9.10	Low	11.65–12.72	Low
Limestone + Fidagran	5.65–5.72	High	6.05–6.08	High	5.53–5.62	Medium-High	5.78–6.03	High	9.95–10.70	Low	13.60–13.80	Low	7.52–9.97	Low	8.50–9.18	Low

† Fertility classes according to Pauletti and Motta (2017): pH – Low (<5.2), Medium (5.2–5.6), High (>5.6); Mn – Low (<16), Medium (16.0–30.0 mg kg^{-1}), High (>30.0 mg kg^{-1}). Values represent the range observed across subplot K sources (phonolite and clayey siltstone) within each main plot treatment.

Data availability

Data will be made available on request

References

Abdel-Fattah, M.K., Mohamed, E.S., Wagdi, E.M., Shahin, S.A., Aldosari, A.A., Lasaponara, R., Alnaimy, M.A., 2021. Quantitative evaluation of soil quality using principal component analysis: the case study of El-Fayoum depression Egypt. Sustainability 13, 1824. https://doi.org/10.3390/su13041824.

Barreto, M.S.C., Elzinga, E.J., Rouff, A.A., Siebecker, M.G., Sparks, D.L., Alleoni, L.R.F., 2024. Zinc speciation in highly weathered tropical soils affected by large scale vegetable production. Sci. Total Environ. 916, 170223. https://doi.org/10.1016/j.scitotenv.2024.170223.

Bassioni, G., Farid, R., Mohamed, M., Hammouda, R.M., Kühn, F.E., 2021. Effect of different parameters on caustic magnesia hydration and magnesium hydroxide rheology: a review. Mater. Adv. 2, 6519–6531. https://doi.org/10.1039/D0MA00887G.

Belgaroui, N., El ifa, W., Hanin, M., 2022. Phytic acid contributes to the phosphate-zinc signaling crosstalk in arabidopsis. Plant Physiol. Biochem. 183, 1–8. https://doi.org/10.1016/j.plaphy.2022.04.029.

Besen, M.R., Ribeiro, R.H., Esper, M., Minato, E.A., Coneglian, C.F., Kachinski, W.D., Tormena, C.A., Inoue, T.T., Batista, M.A., 2021. Lime and phosphogypsum application management: changes in soil acidity, sulfur availability and crop yield. Rev. Bras. Cienc. Solo 45. https://doi.org/10.36783/18069657rbcs20200135.

Borges, C.E., Cazetta, J.O., Sousa, F.B.F. de, Oliveira, K.S., 2020. Aluminum toxicity reduces the nutritional efficiency of macronutrients and micronutrients in sugarcane seedlings. Cienc. E Agrotecnol 44. https://doi.org/10.1590/1413-7054202044015120.

Bouain, N., Shahzad, Z., Rouached, A., Khan, G.A., Berthomieu, P., Abdelly, C., Poirier, Y., Rouached, H., 2014. Phosphate and zinc transport and signalling in plants: toward a better understanding of their homeostasis interaction. J. Exp. Bot. 65, 5725–5741. https://doi.org/10.1093/jxb/eru314.

Brasil, 2016. Instrução Normativa nº 5, de 10 de março de 2016. Regulamentação Das Regras Para Uso Dos Remineralizadores Na Agricultura.

Burbano, D.F.M., Theodoro, S.H., de Carvalho, A.M.X., Ramos, C.G., 2022. Crushed volcanic rock as soil remineralizer: a strategy to overcome the global fertilizer crisis. Nat. Resour. Res. 31, 2197–2210. https://doi.org/10.1007/s11053-022-10107-x.

Chaiwong, N., Bouain, N., Prom-u-thai, C., Rouached, H., 2020. Interplay between silicon and iron signaling pathways to regulate silicon transporter Lsi1 expression in rice. Front. Plant Sci. 11. https://doi.org/10.3389/fpls.2020.01065.

Chen, L., Xue, Y., Wang, N., Gao, H., Hu, G., Liu, J., Cao, L., Zhou, Z., 2025. Soil properties influence the distribution and diversity of plant communities in the desert-loess transition zone. Catena (Amst) 254, 108976. https://doi.org/10.1016/j.catena.2025.108976.

Cruz, L.P., Pacheco, V.S., Silva, L.M., Almeida, R.L., Miranda, M.T., Pissolato, M.D., Machado, E.C., Ribeiro, R.V., 2021. Morpho-physiological bases of biomass production by energy cane and sugarcane: a comparative study. Ind. Crops Prod. 171, 113884. https://doi.org/10.1016/j.indcrop.2021.113884.

de Campos, M., Martello, J.M., de Siqueira, G.F., Garcia, A., Scudeletti, D., Dias, P.P., Rossetto, R., Calonego, J.C., Cantarella, H., Crusciol, C.A.C., 2022. Lime rate in clayey soils influences chemical fertility and sugarcane yield. Plants 11, 2110. https://doi.org/10.3390/plants11162110.

de Carvalho Ribeiro, M., Redondo Martins, A., Silva Alves, R., Frediani Lessa, L.G., Seron Pereira, H., Shintate Galindo, F., Carvalho Minhoto Teixeira Filho, M., Abreu–Junior, C.H., Jani, A.D., Capra, G.F., Ganga, A., Rodrigues Nogueira, T.A., 2025. Basalt rock dust as a soil remineralizer in upland rice grown in tropical soils: residual effects on soil fertility, Si availability, and leaf anatomy. J. Clean. Prod. 520, 146063. https://doi.org/10.1016/j.jclepro.2025.146063.

de Oliveira, D., Borrozzino, E., 2018. Temperatura Do Solo Sob Três Condições De Cobertura Em Londrina, Paranavaí E Guarapuava, No Estado Do Paraná. Agrometeoros 26.

Dong, Y., Yang, J.-L., Zhao, X.-R., Yang, S.-H., Mulder, J., Dörsch, P., Peng, X.-H., Zhang, G.-L., 2022. Soil acidification and loss of base cations in a subtropical agricultural watershed. Sci. Total Environ. 827, 154338. https://doi.org/10.1016/j.scitotenv.2022.154338.

du Toit, D.J.J., Swanepoel, P.A., Hardie, A.G., 2024. Effect of lime source, fineness and granulation on soil permeation with contrasting textures under simulated mediterranean climate rainfall conditions. Commun. Soil Sci. Plant Anal. 55, 3011–3024. https://doi.org/10.1080/00103624.2024.2380485.

Ejigu, W., Selassie, Y.G., Elias, E., Molla, E., 2023. Effect of lime rates and method of application on soil properties of acidic luvisols and wheat (Triticum aestivum, L.) yields in northwest Ethiopia. Heliyon 9, e13988. https://doi.org/10.1016/j.heliyon.2023.e13988.

Emami, N.S., Chavoshi, E., Ayoubi, S., Honarjoo, N., Zeraatpisheh, M., 2024. Comprehensive assessment of soil quality in various land uses: a comparative analysis of soil quality index models. Environ. Earth Sci. 83, 498. https://doi.org/10.1007/s12665-024-11789-7.

Enesi, R.O., Dyck, M., Chang, S., Thilakarathna, M.S., Fan, X., Strelkov, S., Gorim, L.Y., 2023. Liming remediates soil acidity and improves crop yield and profitability - a meta-analysis. Front. Agron. 5. https://doi.org/10.3389/fagro.2023.1194896.

Fuentes, M., Govaerts, B., De León, F., Hidalgo, C., Dendooven, L., Sayre, K.D., Etchevers, J., 2009. Fourteen years of applying zero and conventional tillage, crop rotation and residue management systems and its effect on physical and chemical soil quality. Eur. J. Agron. 30, 228–237. https://doi.org/10.1016/j.eja.2008.10.005.

Goldberg, K., Humayun, M., 2016. Geochemical paleoredox indicators in organic-rich shales of the irati formation, Permian of the Paraná basin, southern Brazil. Braz. J. Geol. 46, 377–393.

Goulding, K.W.T., 2016. Soil acidification and the importance of liming agricultural soils with particular reference to the United Kingdom. Soil Use Manag. 32, 390–399. https://doi.org/10.1111/sum.12270.

Hannam, J.A., Harris, M., Deeks, L., Hoskins, H., Hutchison, J., Withers, A.J., Harris, J. A., Way, L., Rickson, R.J.R., 2025. Developing a multifunctional indicator framework for soil health. Ecol. Indic. 175, 113515. https://doi.org/10.1016/j.ecolind.2025.113515.

Holland, J.E., Bennett, A.E., Newton, A.C., White, P.J., McKenzie, B.M., George, T.S., Pakeman, R.J., Bailey, J.S., Fornara, D.A., Hayes, R.C., 2018. Liming impacts on soils, crops and biodiversity in the UK: a review. Sci. Total Environ. 610–611, 316–332. https://doi.org/10.1016/j.scitotenv.2017.08.020.

Huang, Y.L., Yang, S., Long, G.X., Zhao, Z.K., Li, X.F., Gu, M.H., 2016. Manganese toxicity in sugarcane plantlets grown on acidic soils of southern China. PLoS One 11, e0148956. https://doi.org/10.1371/journal.pone.0148956.

Iqbal, B., Zhou, H., Raheem, A., Inamullah, Zheng, T., Khan, A.R., Azhar, W., Nazir, M.J., Memon, M.S., Li, G., Du, D., 2025. The impact of land use changes and agricultural practices on phosphorus cycling: a review. Land Degrad. Dev. https://doi.org/10.1002/ldr.70221.

Jones, J.D., Mallarino, A.P., 2018. Influence of source and particle size on agricultural limestone efficiency at increasing soil pH. Soil Sci. Soc. Am. J. 82, 271–282. https://doi.org/10.2136/sssaj2017.06.0207.

Kazmierczak, R., Giarola, N.F.B., Riferte, F.B., Santos, J.B. dos, Fogaça, A.M., Carpinelli, S., 2020. Selection of indicators to discriminate soil tillage systems and to assess soil quality in a red latosol. Braz. Arch. Biol. Technol. 63. https://doi.org/10.1590/1678-4324-2020190489.

Khan, A.L., 2025. Silicon: a valuable soil element for improving plant growth and CO2 sequestration. J. Adv. Res. 71, 43–54. https://doi.org/10.1016/j.jare.2024.05.027.

Labanca, E.R.G., Andrade, S.A.L., Kuramae, E.E., Silveira, A.P.D., 2020. The modulation of sugarcane growth and nutritional profile under aluminum stress is dependent on beneficial endophytic bacteria and plantlet origin. Appl. Soil Ecol. 156, 103715. https://doi.org/10.1016/j.apsoil.2020.103715.

Lak, Z.A., Sandén, H., Mayer, M., Godbold, D.L., Rewald, B., 2020. Plasticity of root traits under competition for a nutrient-rich patch depends on tree species and possesses a large congruency between Intra- and interspecific situations. Forests 11, 528. https://doi.org/10.3390/f11050528.

Larkin, R.P., 2020. Effects of selected soil amendments and mulch type on soil properties and productivity in organic vegetable production. Agronomy 10, 795. https://doi.org/10.3390/agronomy10060795.

Li, Y., Cui, S., Chang, S.X., Zhang, Q., 2019. Liming effects on soil pH and crop yield depend on lime material type, application method and rate, and crop species: a global meta-analysis. J. Soils Sediments 19, 1393–1406. https://doi.org/10.1007/s11368-018-2120-2.

Liu, S., Cen, B., Yu, Z., Qiu, R., Gao, T., Long, X., 2025. The key role of biochar in amending acidic soil: reducing soil acidity and improving soil acid buffering capacity. Biochar 7, 52. https://doi.org/10.1007/s42773-025-00432-8.

Liu, S., Qiu, W., Qu, B., Xu, Y., 2010. Dissolution characteristics of limestone with organic acid. In: 2010 4th International Conference on Bioinformatics and Biomedical Engineering. IEEE, pp. 1–4.

López-Hernández, D., Sequera, D., Vallejo, O., Infante, C., 2013. Sugar cane nutrient requirements and the role of atmospheric deposition supplying supplementary fertilization in a Venezuelan sugar cane plantation. Atmósfera 26, 337–348. https://doi.org/10.1016/S0187-6236(13)71080-4.

Luthra, S., Mangla, S.K., Sarkis, J., Tseng, M.-L., 2022. Resources melioration and the circular economy: sustainability potentials for mineral, mining and extraction sector in emerging economies. Resour. Policy 77, 102652. https://doi.org/10.1016/j.resourpol.2022.102652.

Manning, D.A.C., 2018. Innovation in resourcing geological materials as crop nutrients. Nat. Resour. Res. 27, 217–227. https://doi.org/10.1007/s11053-017-9347-2.

Manning, D.A.C., Theodoro, S.H., 2020. Enabling food security through use of local rocks and minerals. Extr. Ind. Soc. 7, 480–487. https://doi.org/10.1016/j.exis.2018.11.002.

Margarita Torres Moreno, M., Raphael da Rocha, R., Hirata Godoy, L., 2014. Major elements geochemistry of sedimentary rocks from Corumbataí formation, Santa gertrudes ceramic pole, S& #227;o paulo, Brazil. Geomaterials 4, 11–17. https://doi.org/10.4236/gm.2014.41002.

Marinari, S., Mancinelli, R., Campiglia, E., Grego, S., 2006. Chemical and biological indicators of soil quality in organic and conventional farming systems in central Italy. Ecol. Indic. 6, 701–711. https://doi.org/10.1016/j.ecolind.2005.08.029.

Martin, T.D., Brockhoff, C.A., Creed, J.T., Long, S.E., 1992. Determination of metals and trace elements in water and wastes by inductively coupled plasma-atomic emission spectrometry. Methods for the Determination of Metals in Environmental Samples, pp. 33–91.

Martins, Silva, D.R.G., Marchi, G., Leite, M.C.A., Martins, É. de S., Gonçalves, A.S.F., Guilherme, L.R.G., 2015. Effect of alternative multinutrient sources on soil chemical properties. Rev. Bras. Cienc. Solo 39, 194–204. https://doi.org/10.1590/01000683rbcs20150587.

Moniz, A.C., Jorge, J.A., Valadares, J., 2009. Métodos De Análise Química, Mineralógica E Física De Solos Do Instituto Agronômico De Campinas.

Moreno-García, B., Casterad, M., Guillén, M., Quílez, D., 2018. Agronomic and economic potential of vegetation indices for rice N recommendations under organic and mineral fertilization in mediterranean regions. Remote Sens. (Basel). 10, 1908.

Nishimoto, M., Kollender, J.P., Muto, I., Hassel, A.W., 2025. In situ ICP-MS analysis of passivation process and selective dissolution of Fe-15Cr alloy in sulfuric acid. Corros. Sci. 249, 112846. https://doi.org/10.1016/j.corsci.2025.112846.

Ofoe, R., Thomas, R.H., Asiedu, S.K., Wang-Pruski, G., Fofana, B., Abbey, Lord, 2023. Aluminum in plant: benefits, toxicity and tolerance mechanisms. Front. Plant Sci. 13. https://doi.org/10.3389/fpls.2022.1085998.

Omara-Ojungu, C., Lukac, M., 2025. Effects of MicroChar on phosphorus availability and pea growth. J. Soil Sci. Plant Nutr. 25, 5934–5948. https://doi.org/10.1007/s42729-025-02508-7.

Panalytical, B.V., 2002. X'pert highscore plus. X'Pert HighScore Plus, Lelyweg, Almelo, the Netherlands 2.

Pauletti, V., Motta, A.C.V., 2017. Manual De Adubação E Calagem Para O Estado Do Paraná. Sociedade Brasileira de Ciência do Solo, Núcleo Estadual Paraná, Curitiba.

Pierpaoli, E., Carli, G., Pignatti, E., Canavari, M., 2013. Drivers of precision agriculture technologies adoption: a literature review. Procedia Technol. 8, 61–69. https://doi.org/10.1016/j.protcy.2013.11.010.

Ramos, C.G., Querol, X., Oliveira, M.L.S., Pires, K., Kautzmann, R.M., Oliveira, L.F.S., 2015. A preliminary evaluation of volcanic rock powder for application in agriculture as soil a remineralizer. Sci. Total Environ. 512, 371–380. https://doi.org/10.1016/j.scitotenv.2014.12.070.

Rauch, H.W., White, W.B., 1977. Dissolution kinetics of carbonate rocks: 1. Effects of lithology on dissolution rate. Water Resour. Res. 13, 381–394.

Richardson, J.B., 2024. Basalt rock dust amendment on soil health properties and inorganic nutrients—laboratory and field study at two organic farm soils in new England, USA. Agriculture 15, 52. https://doi.org/10.3390/agriculture15010052.

Rodrigues, M., da Silva Junges, L.F., Mozorovicz, C., Seidel Ziemmer, G., Kosera Neto, C., Américo de Andrade, E., Izabel dos Passos, A., Palczewski Pacheco, F., Cezar, E., de Melo Teixeira, L., 2024a. Paraná basin basalt powder: a multinutrient soil amendment for enhancing soil chemistry and microbiology. J. South Am. Earth Sci. 141, 104957. https://doi.org/10.1016/j.jsames.2024.104957.

Rodrigues, M., Nanni, M.R., Posser Silveira, C.A., Cezar, E., Leboso Alemparte Abrantes dos Santo, G., Herrig Furlanetto, R., de Oliveira, K.M., Silveira Reis, A., 2021a. Mining Co-products as sources of multi-nutrients for cultivation of Brachiaria ruziziensis. Nat. Resour. Res. 30, 849–865. https://doi.org/10.1007/s11053-020-09745-w.

Rodrigues, M., Nanni, M.R., Posser Silveira, C.A., Gualberto, A.A. da S., 2021b. Mining coproducts as alternative sources of nutrients for the cultivation of sugarcane (Saccharum officinarum). J. Clean. Prod. 291, 125925. https://doi.org/10.1016/j.jclepro.2021.125925.

Rodrigues, M., Silveira, C.A.P., Cezar, E., de Oliveira, R.B., Reis, A.S., dos Santos, G.L.A. A., de Melo Teixeira, L., Nanni, M.R., 2024b. Enhancing soybean cultivation sustainability: impact of limestone mining co-products on soil and plant chemical attributes. Discov. Agricult. 2, 50. https://doi.org/10.1007/s44279-024-00072-9.

Rodrigues, M., Vahl, L.C., Posser Silveira, C.A., Mamudo Salé, M., Batista, M.A., Nanni, M.R., 2023. Limestone mining By-Product as a source of nutrients for the cultivation of onion (*Allium Cepa* L.). Commun. Soil Sci. Plant Anal. 54, 2683–2698. https://doi.org/10.1080/00103624.2023.2240371.

Rodrigues, M., Vahl, L.C., Silveira, C.A.P., Salé, M.M., Nanni, M.R., Batista, M.A., 2021c. Co-products from the limestone mining as sources of calcium, magnesium and sulphur. Environ. Nanotechnol. Monit. Manag. 15, 100446. https://doi.org/10.1016/j.enmm.2021.100446.

Russell, M.D., Heckman, K.A., Pan, L., Ye, X., Zalesny, R.S., Kane, E.S., 2024. Mine waste rock as a soil amendment for enhanced weathering, ecosystem services, and bioenergy production. Front. Earth Sci. (Lausanne). 12. https://doi.org/10.3389/feart.2024.1414437.

Saenchai, C., Bouain, N., Kisko, M., Prom-u-thai, C., Doumas, P., Rouached, H., 2016. The involvement of OsPHO1;1 in the regulation of iron transport through integration of phosphate and zinc deficiency signaling. Front. Plant Sci. 7. https://doi.org/10.3389/fpls.2016.00396.

Salgado, L., Aparicio, L., Afif, E., Fernández-López, E., Gallego, J.R., Forján, R., 2024. A second life for mining waste as an amendment for soil remediation. J. Mater. Cycles Waste Manag. 26, 2971–2979. https://doi.org/10.1007/s10163-024-02013-6.

Saliu, M.A., Shehu, S.A., 2012. Effects of calcite and dolomite mining on water and soil qualities: a case study of freedom group of companies, Ikpeshi, Edo state Nigeria. J. Emerg. Trends Eng. Appl. Sci. 3, 19–24.

Shoemaker, H.E., McLean, E.O., Pratt, P.F., 1961. Buffer methods for determining lime requirement of soils with appreciable amounts of extractable aluminum. Soil Sci. Soc. Am. J. 25, 274–277.

Silva, E. de B., Souza, W.C.L. de, Nardis, B.O., Alleoni, L.R.F., Grazziotti, P.H., Santos, L. L. dos, Bezerra, I.R.S., Alves, F.A.F., Silva, W.C., Uane, B.G., Nascimento, S.A. do, 2024. Toxicity and availability of manganese in the growth of tropical grasses in contaminated soil. Appl. Environ. Soil Sci. https://doi.org/10.1155/2024/7444193.

Silva, F.C.D.A.S., 2009. Manual De Análises Químicas De Solos, Plantas E Fertilizantes. Embrapa Informação Tecnológica, Rio de Janeiro. Embrapa Solos Brasília.

Skov, K., Wardman, J., Healey, M., McBride, A., Bierowiec, T., Cooper, J., Edeh, I., George, D., Kelland, M.E., Mann, J., Manning, D., Murphy, M.J., Pape, R., Teh, Y.A., Turner, W., Wade, P., Liu, X., 2024. Initial agronomic benefits of enhanced weathering using basalt: a study of spring oat in a temperate climate. PLoS One 19, e0295031. https://doi.org/10.1371/journal.pone.0295031.

Smith, D.K.D.K., Jenkins, R., 1996. The powder diffraction file: past, present, and future. J. Res. Natl. Inst. Stand. Technol. 101, 259. https://doi.org/10.6028/jres.101.027.

Srbinovska, M., Gavrovski, C., Dimcev, V., Krkoleva, A., Borozan, V., 2015. Environmental parameters monitoring in precision agriculture using wireless sensor networks. J. Clean. Prod. 88, 297–307. https://doi.org/10.1016/j.jclepro.2014.04.036.

Teixeira, P.C., Donagemma, G.K., Fontana, A., Teixeira, W.G., 2017. Manual De Métodos De Análise De Solo. Embrapa, Rio de Janeiro, p. 573p.

Testoni, S.A., Prandel, L.V., Melo, V.F., Dawson, L.A., da Silva Salvador, F.A., 2022. Conjunctive use of synchrotron x-ray diffraction and rietveld refinement in Fe-oxide clays for forensic applications. J. Forensic Sci. 67, 2020–2031. https://doi.org/10.1111/1556-4029.15098.

Thorburn, P.J., Biggs, J.S., Webster, A.J., Biggs, I.M., 2011. An improved way to determine nitrogen fertiliser requirements of sugarcane crops to meet global environmental challenges. Plant Soil 339, 51–67. https://doi.org/10.1007/s11104-010-0406-2.

van Straaten, P., 2007. Agrogeology: the Use of Rocks for Crops. Enviroquest, Ontario, CA.

Wenyika, P., Enesi, R.O., Gorim, L.Y., Dyck, M., 2025. Effects of liming on soil physical and chemical properties in Europe and North America: a review. Agrosystems. Geosci. & Environ. 8. https://doi.org/10.1002/agg2.70175.

WRB., 2015. World reference base for soil resources 2014, update 2015: International soil classification system for naming soils and creating legends for soil maps, 106. World Soil Resources Reports No, Rome.

Yasuda, E.Y., Santos, R.G. dos, Vidal Trevisan, O., 2013. Kinetics of carbonate dissolution and its effects on the porosity and permeability of consolidated porous media. J. Pet. Sci. Eng. 112, 284–289. https://doi.org/10.1016/j.petrol.2013.11.015.

Yuan, X., Luo, Y., Liang, R., Ma, L., Ren, X., He, T., Liang, Y., Chen, B., Wang, Z., Yao, W., 2025. Neutral soil supports better growth and productivity of sugarcane (Saccharum officinarum L.) than acidic soil in China. J. Agric. Food Res. 23, 102265. https://doi.org/10.1016/j.jafr.2025.102265.

Zambrosi, F.C.B., Mesquita, G.L., Marchiori, P.E.R., Tanaka, F.A.O., Machado, E.C., Ribeiro, R.V., 2016. Anatomical and physiological bases of sugarcane tolerance to manganese toxicity. Environ. Exp. Bot. 132, 100–112. https://doi.org/10.1016/j.envexpbot.2016.08.011.